128. Newman RM, Hall L, Kirmaier A, *et al.* Evolution of a TRIM5-CypA splice isoform in old world monkeys. *PLoS Pathog* 2008; **4**: e1000003.
129. Wilson SJ, Webb BL, Ylinen LM, Verschoor E, Heeney JL, Towers GJ. Independent evolution of an antiviral TRIMCyp in rhesus macaques. *Proc Natl Acad Sci USA* 2008; **105**: 3557–3562.
130. Hatziioannou T, Ambrose Z, Chung NP, *et al.* A macaque model of HIV-1 infection. *Proc Natl Acad Sci USA* 2009; **106**: 4425–4429.
131. Keeble AH, Khan Z, Forster A, James LC. TRIM21 is an IgG receptor that is structurally, thermodynamically, and kinetically conserved. *Proc Natl Acad Sci USA* 2008; **105**: 6045–6050.

ARTICLE IN PRESS

YVIRO-05587; No. of pages: 9; 4C: 3

Virology xxx (2010) xxx–xxx

Contents lists available at ScienceDirect

Virology

journal homepage: www.elsevier.com/locate/yviro

Contribution of RING domain to retrovirus restriction by TRIM5α depends on combination of host and virus

Hikoichiro Maegawa, Tadashi Miyamoto, Jun-ichi Sakuragi, Tatsuo Shioda, Emi E. Nakayama *

Department of Viral Infections, Research Institute for Microbial Diseases, Osaka University, 3-1, Yamadaoka, Suita-shi, Osaka 565-0871, Japan

ARTICLE INFO

Article history:
Received 19 October 2009
Returned to author for revision
8 November 2009
Accepted 5 January 2010
Available online xxxx

ABSTRACT

The anti-retroviral restriction factor TRIM5α contains the RING domain, which is frequently observed in E3 ubiquitin ligases. It was previously proposed that TRIM5α restricts human immunodeficiency virus type 1 (HIV-1) via proteasome-dependent and -independent pathways. Here we examined the effects of RING domain mutations on retrovirus restriction by TRIM5α in various combinations of virus and host species. Simian immunodeficiency virus isolated from macaque (SIVmac) successfully avoided attacks by RING mutants of African green monkey (AGM)-TRIM5α that could still restrict HIV-1. Addition of proteasome inhibitor did not affect the anti-HIV-1 activity of AGM-TRIM5α, whereas it disrupted at least partly its anti-SIVmac activity. In the case of mutant human TRIM5α carrying proline at the position 332, however, both HIV-1 and SIVmac restrictions were eliminated as a result of RING domain mutations. These results suggested that the mechanisms of retrovirus restriction by TRIM5α vary depending on the combination of host and virus.

Introduction

Replication of retroviruses is influenced by several factors in host cells. Tripartite motif protein (TRIM) 5α has been identified as a restriction factor of human immunodeficiency virus type 1 (HIV-1) in rhesus monkey (Rh) cells (Stremlau et al., 2004). Rh TRIM5α potently restricts HIV-1 but only weakly does so simian immunodeficiency virus isolated from macaque (SIVmac) (Stremlau et al., 2004; Song et al., 2005), whereas African green monkey (AGM) TRIM5α can potently restrict both HIV-1 and SIVmac (Nakayama et al., 2005; Song et al., 2005). TRIM5α consists of the RING, B-box 2, coiled-coil, and SPRY (B30.2) domains (Reymond et al., 2001). Differences in the amino acid sequences in the SPRY domain of TRIM5α of different monkey species were shown to affect the species-specific restriction of retrovirus infection (Perez-Caballero et al., 2005a; Nakayama et al., 2005; Sawyer et al., 2005; Stremlau et al., 2005; Yap et al., 2005). In addition, biochemical studies have shown that TRIM5α associates with retroviral capsid (CA) protein in detergent-stripped virions or with an artificially constituted core structure composed of capsid–nucleocapsid (CA–NC) fusion protein in a SPRY domain-dependent manner (Sebastian and Luban, 2005; Stremlau et al., 2006a). The SPRY domain is thus thought to recognize viral core. The coiled-coil domain of TRIM5α is important for the formation of homo-oligomers (Mische et al., 2005) and is essential for antiviral activity (Javanbakht et al., 2006). The intact B-box 2 domain is also required for TRIM5α mediated antiviral activity, since the restrictive activity of TRIM5α is diminished by amino acid substitutions in the B-box 2 domain (Javanbakht et al., 2005). RING containing proteins were frequently found to possess E3 ubiquitin ligase activity (Jackson et al., 2000). Indeed, Rh TRIM5α was poly-ubiquitinated and degraded rapidly via the ubiquitin-proteasome pathway, while disruption of the RING domain eliminated its auto-ubiquitination (Diaz-Griffero et al., 2006). Furthermore, it was demonstrated that TRIM5α is degraded via the ubiquitin-proteasome pathway during HIV-1 restriction (Rold and Aiken, 2008). However, deletion of the RING domain in TRIM5α only partially attenuates anti-HIV-1 activity (Javanbakht et al., 2005; Perez-Caballero et al., 2005b). Moreover, modulation of E1 ubiquitin-activating enzyme expression did not affect TRIM5α-mediated restriction activity in a temperature-dependent cell line (Perez-Caballero et al., 2005b) and finally, proteasome inhibitors did not affect TRIM5α mediated HIV-1 restriction (Anderson et al., 2006; Perez-Caballero et al., 2005b; Rold and Aiken, 2008; Stremlau et al., 2006a; Wu et al., 2006) even though they allowed HIV-1 to generate viral late reverse transcripts under TRIM5α mediated HIV-1 restriction (Anderson et al., 2006; Wu et al., 2006). The exact role of the TRIM5α RING domain in retrovirus restriction thus remains unclear.

In the study presented here, we investigated the effects of RING domain mutations on HIV-1 and SIVmac restrictions by TRIM5α and report that TRIM5α restricts HIV-1 and SIVmac differently.

* Corresponding author. Fax: +81 6 6879 8347.
E-mail address: emien@biken.osaka-u.ac.jp (E.E. Nakayama).

0042-6822/$ – see front matter © 2009 Published by Elsevier Inc.
doi:10.1016/j.virol.2010.01.003

Results

Auto poly-ubiquitination of TRIM5α impaired by mutations in RING domain

The RING finger domain of TRIM5α comprises eight potential metal ligands and binds two atoms of zinc, with each zinc atom ligated tetrahedrally by either four cysteins or three cysteines and a single histidine. Based on the three-dimensional structure of the RING domains of TRIM5 (Abe et al., 2007) and the promyelocytic leukemia (PML) protein (Borden et al., 1995; Borden and Freemont, 1996), the first pair of metal ligands of the AGM TRIM5α RING domain (C15 and C18) would share a zinc atom with the third pair (C35 and C38), and the second (C30 and H32) and fourth pairs (C56 and C59) would share another zinc atom (Fig. 1A). To determine whether anti-HIV-1 and anti-SIVmac activities of AGM TRIM5α are similarly affected by RING domain mutations, several AGM TRIM5α constructs with mutations in the RING domain were generated (Fig. 1B). In the mutant TRIM5α constructs with C15AC18A, C30AH32A, or C15AC18AC30AH32A, two key amino acid residues in the first or second, or in both the first and

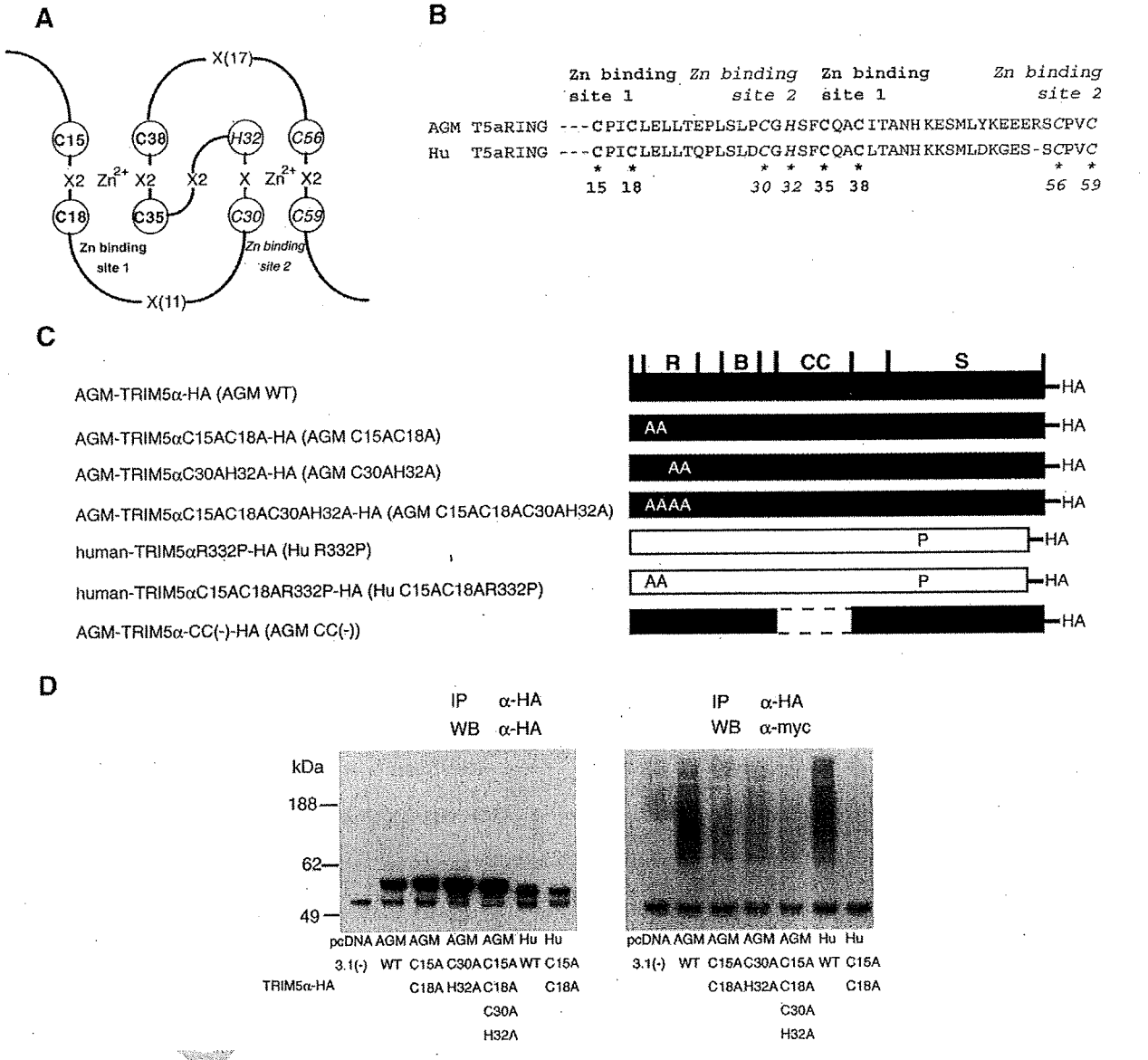

Fig. 1. Auto poly-ubiquitination of TRIM5α was impaired by RING domain mutations. (A) The RING finger zinc binding motif. The numbered AGM TRIM5α zinc-binding ligands are shown in circles. Each zinc atom is coordinated tetrahedrally by four ligands. Zinc-binding site 1 (**bold**) and site 2 (*italic*) are indicated. The numbers of amino acid residues between the zinc-binding cystein and histidine ligands in AGM TRIM5α are also indicated. (B) Primary amino acid sequences of the RING domains of AGM TRIM5α (AGM T5aRING) and human TRIM5α (Hu T5aRING) are aligned. Zinc-binding site 1 (**bold**), site 2 (*italic*), and cystein and histidine ligands (large numbers) are indicated. (C) Schematic representation of TRIM5α constructs. Black and white bars denote AGM and Hu sequences, respectively. Abbreviations for domains: R, RING; B, B-box 2; CC, Coiled-coil; S, SPRY. A dotted box denotes deletion of corresponding amino acid. The positions of individual amino acid changes are also indicated. (D) 293 T cells were transfected with plasmids encoding HA-tagged AGM TRIM5α (TRIM5α-HA) or its RING mutants together with a plasmid expressing myc-tagged ubiquitin (myc-Ub). Forty-eight hours after transfection, the cells were lysed and TRIM5α proteins in the lysates were precipitated with an anti-HA antibody. The immunoprecipitates were Western blotted and probed with anti-HA antibody for TRIM5α detection or with anti-myc antibody for ubiquitin detection. Abbreviations: WB, Western blot; IP, immunoprecipitation. The representative results of two independent experiments with similar results are shown.

Please cite this article as: Maegawa, H., et al., Contribution of RING domain to retrovirus restriction by TRIM5α depends on combination of host and virus, Virology (2010), doi:10.1016/j.virol.2010.01.003

second zinc-binding sites within the RING domain of AGM TRIM5α were replaced with alanine residues, respectively. All mutant TRIM5α constructs contained the HA-tag at their C-terminus (Fig. 1C).

To determine the effects of TRIM5α RING mutations on its ubiquitin ligase activity, 293 T cells were transfected with plasmids encoding HA-tagged TRIM5αs together with plasmid expressing myc tagged ubiquitin. Forty-eight hours later, the cells were lysed and TRIM5α proteins were precipitated with the anti-HA antibody followed by Western blot analysis using anti-HA and anti-myc antibodies. Poly-ubiquitinated forms of the wild type AGM TRIM5α were observed (Fig. 1D). AGM TRIM5α with C15AC18A or C30AH32A was less poly-ubiquitinated than the wild type AGM TRIM5α, and AGM TRIM5α with C15AC18AC30AH32A was the least poly-ubiquitinated among the mutant constructs tested. These results confirmed the previously published report (Diaz-Griffero et al., 2006) that the TRIM5α RING zinc-binding site mutations impaired auto poly-ubiquitination of TRIM5α.

Contribution of RING domain to retrovirus restriction by AGM TRIM5α

We next examined anti-viral activities of zinc-binding site mutants of TRIM5α. The HA-tagged wild type and mutant AGM TRIM5α proteins were expressed by SeVs in MT4 cells (Fig. 2A). CV1 cells were then used for a confocal microscopic examination of cytoplasmic bodies, since the cytoplasm of MT4 cells is not large enough for observation of cytoplasmic bodies. Each of the TRIM5αs with RING mutations formed uniformly larger cytoplasmic bodies than did the wild type (Fig. 2B), although the size of cytoplasmic bodies slightly

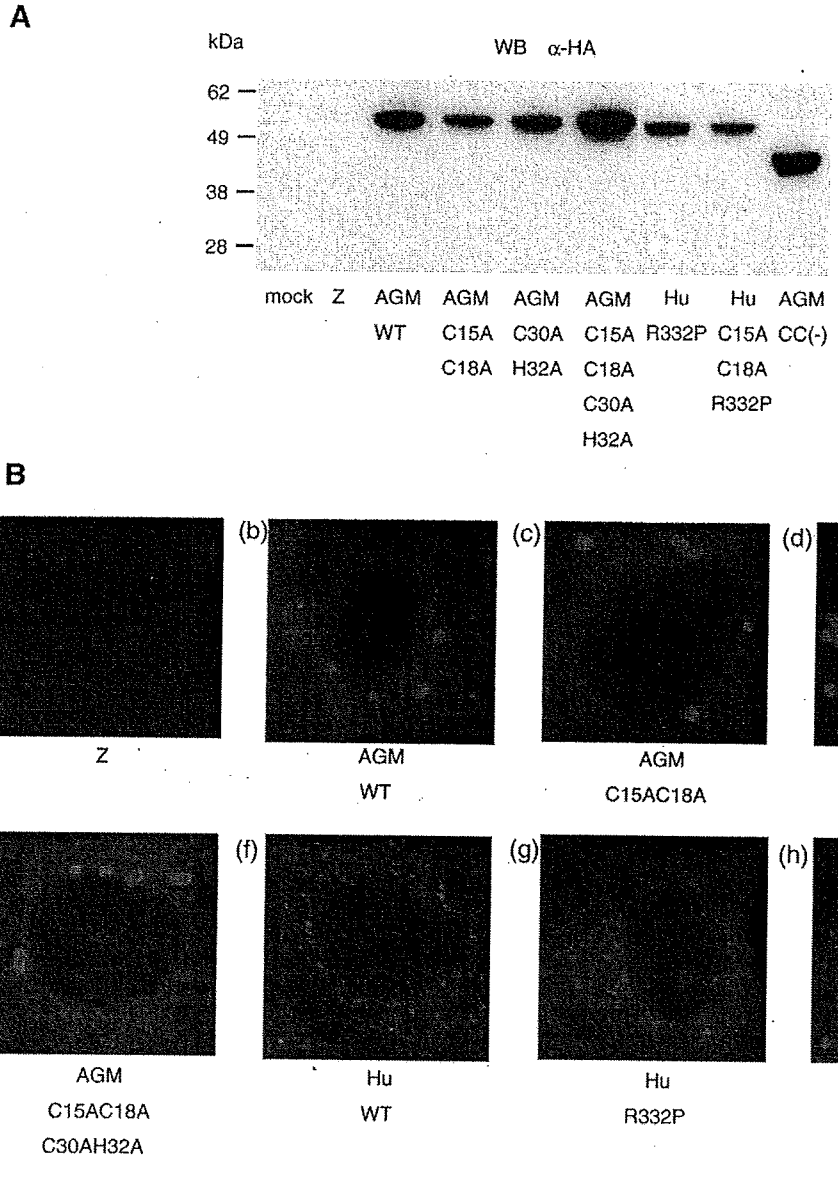

Fig. 2. Expression of RING mutant TRIM5α proteins. (A) Expression of various TRIM5αs. TRIM5α proteins in MT4 cells mock infected (mock) or infected with parental Z strain of SeV (Z), SeVs expressing AGM TRIM5α (AGM WT), AGM TRIM5α C15AC18A (AGM C15AC18A), AGM TRIM5α C30AH32A (AGM C30AH32A), AGM TRIM5α C15AC18AC30AH32A (AGM C15AC18AC30AH32A), human TRIM5α R332P (Hu R332P), human TRIM5α C15AC18AR332P (Hu C15AC18AR332P), or AGM-TRIM5α-Coiled-coil(—) (AGM CC(—)), were visualized by Western blotting with antibody to HA. (B) Subcellular localization of TRIM5αs. CV1 cells infected with SeV expressing HA-tagged TRIM5 proteins were analyzed as described in "Materials and methods". Representative confocal microscopic images are shown of parental Z strain of SeV (a), or with SeV expressing AGM WT (b), AGM C15AC18A (c), AGM C30AH32A (d), AGM C15AC18AC30AH32A (e), Hu WT (f), Hu R332P (g), or Hu C15AC18AR332P (h).

Please cite this article as: Maegawa, H., et al., Contribution of RING domain to retrovirus restriction by TRIM5α depends on combination of host and virus, Virology (2010), doi:10.1016/j.virol.2010.01.003

varied among different RING mutants of TRIM5α. These results confirmed the previous observations on Rh TRIM5α (Javanbakht et al., 2005). Specifically, AGM TRIM5α with C30AH32A showed the highest numbers of cytoplasmic bodies and the least levels of diffuse staining of cytoplasm among the three RING mutants (Fig. 2B).

For the viral replication assay, MT4 cells infected with SeVs expressing the wild type and mutant TRIM5αs were also superinfected with the NL43 strain of HIV-1, GH123 strain of HIV-2 or SIVmac239. Three days after infection, culture supernatants were collected and assayed for their levels of p24, p25 or p27 viral CA protein, respectively. AGM-TRIM5α-CC(−) was used as a negative control. AGM TRIM5α with C15AC18A, C30AH32A, or C15AC18A-C30AH32A moderately inhibited HIV-1 growth, while these variants completely lost their inhibitory effect on SIVmac growth (Fig. 3A). These results indicated that effects of cysteine substitutions in RING domain on anti-HIV-1 activity of AGM TRIM5α differ from those on anti-SIVmac activity, suggesting that SIVmac restriction by AGM TRIM5α was totally dependent on the intact RING domain of TRIM5α, while HIV-1 restriction was at least in part independent from this domain as reported previously (Javanbakht et al., 2005; Perez-Caballero et al., 2005b; Stremlau et al., 2004). It has been proposed that both proteasome-dependent and -independent pathways are involved in HIV-1 restriction by Rh TRIM5α, since disrupting the proteasome function by adding a proteasome inhibitor enabled the generation of normal levels of HIV-1 late reverse transcribed products, although HIV-1 infection and the generation of nuclear imports of 1-LTR and 2-LTR viral cDNA forms remained impaired by Rh TRIM5α (Anderson et al., 2006; Wu et al., 2006). We therefore concluded that AGM TRIM5α restricts SIVmac mainly via the RING-proteasome-dependent pathway.

We then tested the third virus, human immunodeficiency virus type 2 (HIV-2), which is more closely related to SIVmac than to HIV-1 (Gao et al., 1999). AGM TRIM5α clearly inhibited HIV-2 GH123 replication and all the RING domain mutants showed reduced anti-HIV-2 activity. AGM TRIM5α with C30AH32A completely lost its anti-HIV-2 activity (Fig. 3A). Unlike SIVmac, however, AGM TRIM5α with C15AC18A or C15AC18AC30AH32A still moderately inhibited HIV-2 GH123 growth (Fig. 3A). These results indicate that the RING domain contribution to HIV-2 restriction by TRIM5α was also distinct from its contributions to HIV-1 and SIVmac restrictions.

In a single round infection assay, MT4 cells infected with SeVs expressing the wild type or mutant TRIM5αs variants were superinfected with HIV-1-GFP or SIVmac-GFP. The wild type AGM TRIM5α potently restricted both HIV-1-GFP and SIVmac-GFP infection (Fig. 3B) as reported previously (Nakayama et al., 2005). On the other hand, AGM TRIM5α with C15AC18A, C30AH32A, or C15AC18A-C30AH32A only moderately inhibited HIV-1-GFP infection, while these variants completely lost their inhibitory effect on SIVmac-GFP infection (Fig. 3B). AGM C30AH32A exhibited the weakest anti-HIV-1 activity among the generated mutant constructs, probably due to its limited localization within the cytoplasm. However, the number of HIV-1-infected cells was still lower in AGM C30AH32A expressing cells than in those expressing negative control AGM-TRIM5α-CC(-) or cells infected with the parental SeV Z strain (Fig. 3B). The same results as above were obtained when we use canine Cf2Th cell line lacking endogenous TRIM5α expression (Sawyer et al., 2007) (Fig. 3C). These results confirmed our results in viral replication assay described in Fig. 3A.

Contribution of RING domain to retrovirus restriction by human TRIM5α with arginine-to-proline substitution at the 332nd position

An arginine-to-proline substitution at the 332nd position (R332P) in the SPRY domain reportedly conferred strong anti-HIV-1 and anti-SIVmac activities to human TRIM5α (Stremlau et al., 2005; Yap et al., 2005). To determine whether cystein residue substitutions in the RING domain of human TRIM5α with R332P (Hu-R332P) have similar effects on its anti-HIV-1 and anti-SIVmac activities to those of AGM TRIM5α described above, C15AC18A substitutions were introduced in Hu-R332P. The protein expression levels of Hu-R332P with C15AC18A were comparable to those of Hu-R332P without C15AC18A (Fig. 2B). In addition, Hu-R332P inhibited both HIV-1 and SIVmac infection (Fig. 3A, B and C), which confirmed previous findings (Stremlau et al., 2005; Yap et al., 2005). As expected, Hu-R332P with C15AC18A completely lost its auto poly-ubiquitination (Fig. 1D) and anti-SIVmac activity (Fig. 3A, B and C) indicating that SIVmac restriction by Hu-R332P also strongly depends on the intact RING domain of TRIM5α. In contrast to AGM TRIM5α, however, Hu-R332P with C15AC18A completely lost its anti-HIV-1 activity (Fig. 3A, B and C). These findings suggest that, unlike AGM TRIM5α, Hu-R332P TRIM5α restricted both HIV-1 and SIVmac mainly via a RING-proteasome-dependent pathway. Hu-R332P TRIM5α with C15AC18A also failed to restrict HIV-2 GH123 (Fig. 3A). Taken together with results on AGM TRIM5α described above, our results indicated that the extent of RING domain contribution to retrovirus restriction by TRIM5α could be determined by a combination of virus and host species. We speculate that the intact RING domain is required for the proteasome-dependent but not for the proteasome-independent pathway of TRIM5α restriction of retroviruses.

Effect of proteasome inhibition on antiviral activity of TRIM5α

For a direct investigation of whether AGM TRIM5α restricts SIVmac and Hu-R332P TRIM5α restricts both HIV-1 and SIVmac mainly via proteasome-dependent pathway, we used a proteasome inhibitor MG132. MT4 cells infected with SeVs expressing various TRIM5α were superinfected with HIV-1-GFP or SIVmac-GFP in the presence or absence of MG132. After infection, the cells were thoroughly washed and incubated in MG132-free medium. As shown in Fig. 4, MG132 had no effect at all on the anti-HIV-1 activity of AGM, Rh or cynomolgus monkey and of human/AGM chimeric TRIM5α carrying the SPRY domain of AGM TRIM5α and the RING, B-box 2, and coiled-coil domains of human TRIM5α. In contrast, and as expected, MG132 at least partially disrupted the anti-HIV-1 activity of Hu-R332P TRIM5α. Rh and cynomolgus monkey TRIM5α could not restrict SIVmac infection and that addition of MG132 did not affect the numbers of GFP-positive cells, indicating that the condition for MG132 treatment used in our study did not affect cell viability (Fig. 4). AGM, Hu-R332P and human/AGM chimeric TRIM5α restricted SIVmac infection while MG132 partially disrupted the anti-SIVmac activity of those TRIM5α. When we used Cf2Th cells, MG132 also disrupted the anti-HIV-1 activity of Hu-R332P TRIM5α at least

Fig. 3. Contribution by RING domain to retrovirus restriction by TRIM5α depends on combination of host and viral species. (A) MT4 cells were infected with SeV expressing AGM CC (−), AGM WT, AGM C15AC18A, AGM C30AH32A, AGM C15AC18AC30AH32A, Hu R332P, or Hu C15AC18AR332P. The cells were then superinfected with HIV-1 NL43, HIV-2 GH123 or SIVmac239. The culture supernatants were collected three days after infection for measurement of the p24, p25 or p27 levels. The representative results of two independent experiments with similar results are shown. Error bars denote actual fluctuations of duplicate samples. (B) MT4 cells were infected with parental Z strain of SeV (crosses), or with SeVs expressing AGM WT (black squares), AGM CC(−) (white squares), AGM C15AC18A (black triangles), AGM C30AH32A (white triangles), AGM C15AC18AC30AH32A (white diamonds), Hu R332P (black circles), or Hu C15AC18AR332P (white circles). The cells were then superinfected with serially diluted HIV-1-GFP or SIVmac-GFP. The representative results of two independent experiments with similar results are shown. (C) Canine Cf2Th cells were infected with SeVs expressing indicated TRIM5α protein. The cells were then superinfected with HIV-1-GFP or SIVmac-GFP. The representative results of four independent experiments with similar results are shown. Error bars denote standard deviation in triplicate samples.

Please cite this article as: Maegawa, H., et al., Contribution of RING domain to retrovirus restriction by TRIM5α depends on combination of host and virus, Virology (2010), doi:10.1016/j.virol.2010.01.003

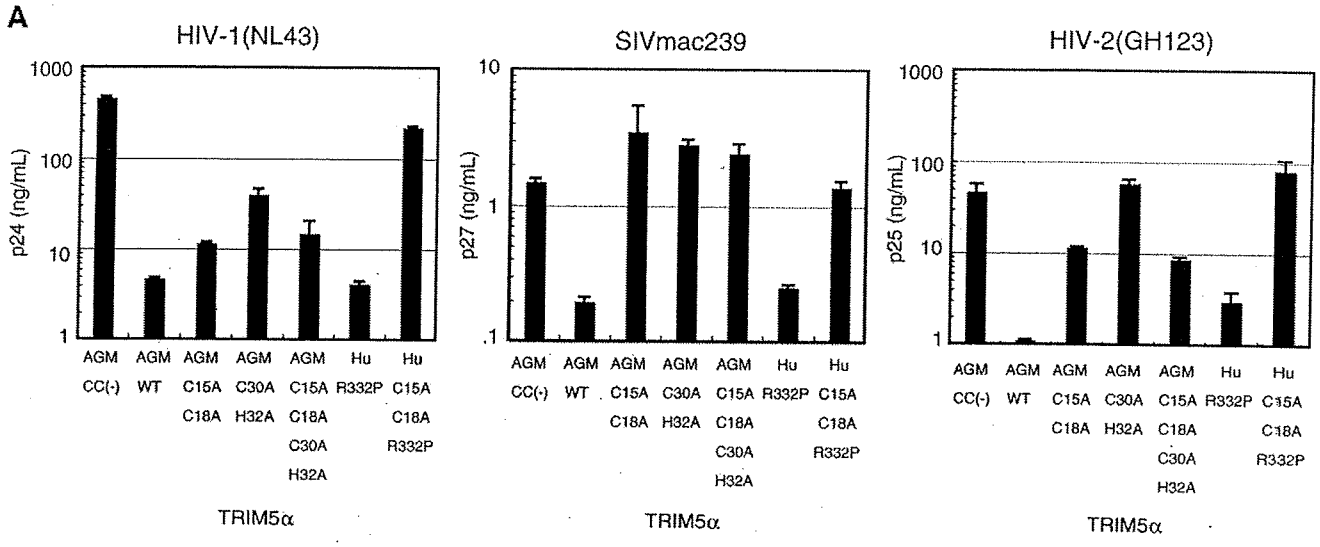

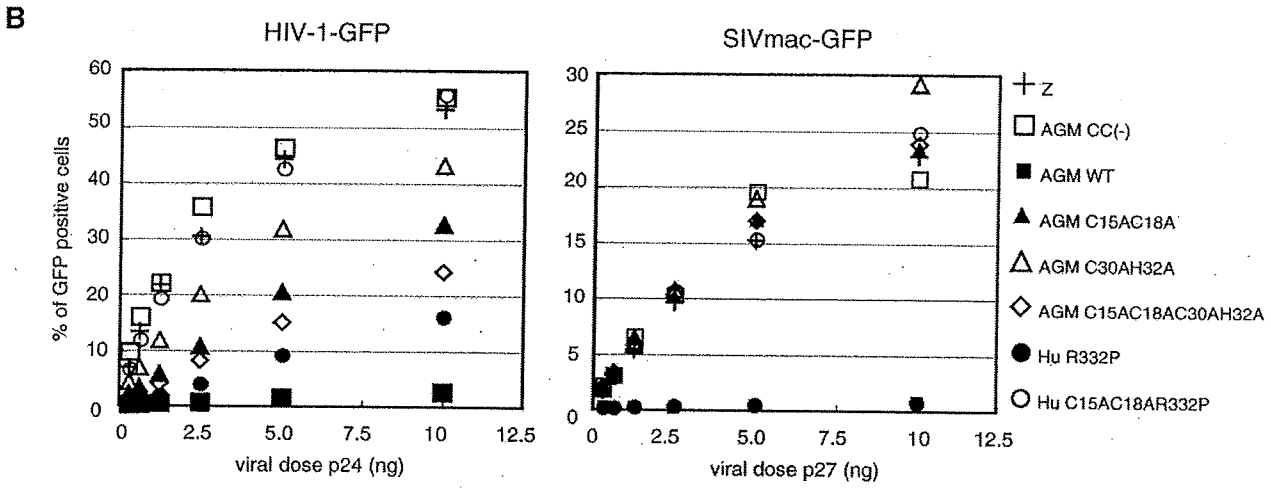

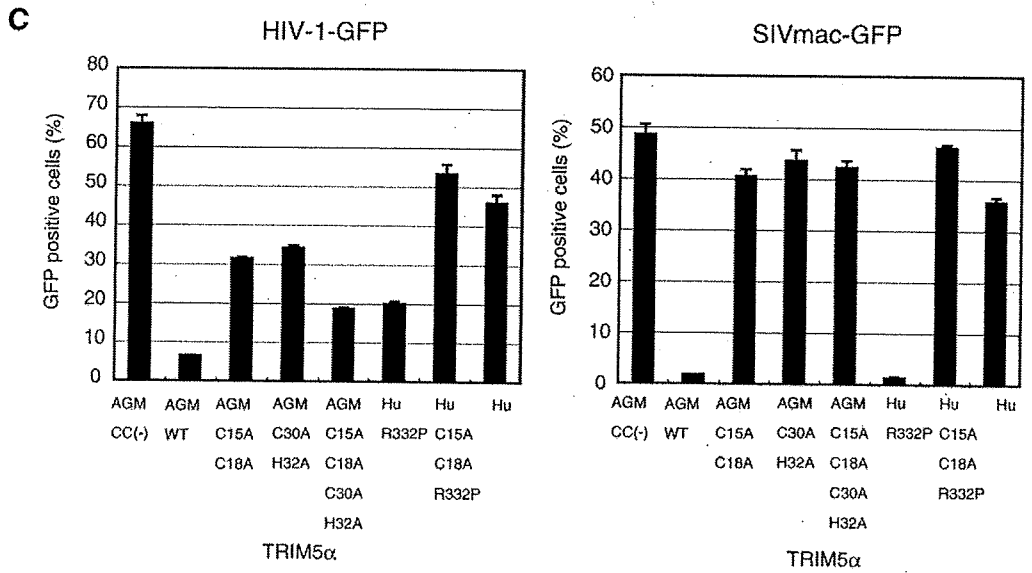

Please cite this article as: Maegawa, H., et al., Contribution of RING domain to retrovirus restriction by TRIM5α depends on combination of host and virus, Virology (2010), doi:10.1016/j.virol.2010.01.003

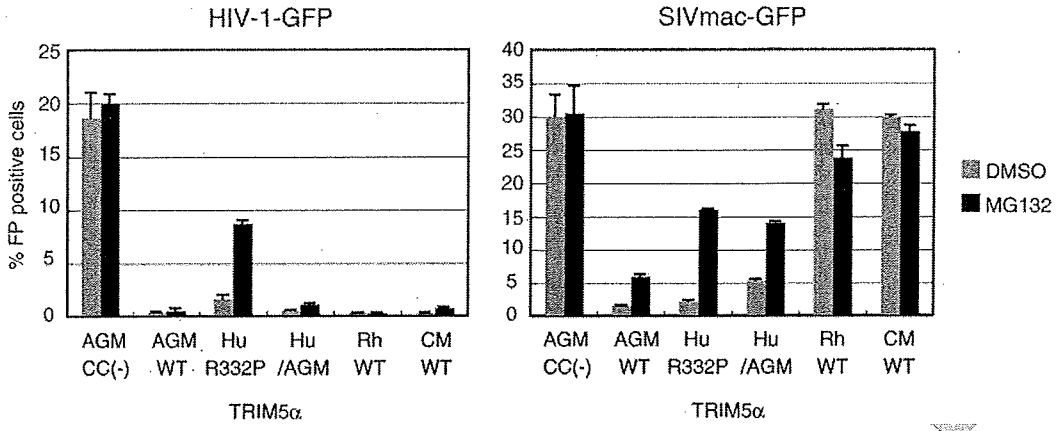

Fig. 4. The effect of proteasome inhibition on antiviral activity of TRIM5α depends on combinations of TRIM5α and viruses. MT4 cells were infected with SeVs expressing AGM CC (−), AGM WT, Hu R332P, Hu/AGM, Rh WT or CM WT. Cells were then superinfected with HIV-1-GFP or SIVmac-GFP in the presence of 10 μM MG132 in 0.1% DMSO (black bar) or 0.1% DMSO (gray bar). The representative results of three independent experiments with similar results are shown. Error bars denote actual fluctuations of duplicate samples.

partially (data not shown). These results support our conclusions that AGM TRIM5α restricted SIVmac mainly via the proteasome-dependent pathway, and that Hu-R332P TRIM5α restricted both HIV-1 and SIVmac mainly via the proteasome-dependent pathway (see Table 1 for summary of these results).

As described above, the previous studies have shown that disrupting the proteasome function by adding a proteasome inhibitor enabled the generation of HIV-1 late reverse transcribed products, even though HIV-1 infection and the generation of nuclear imports of 1-LTR and 2-LTR viral cDNA forms remained impaired by Rh TRIM5α (Anderson et al., 2006; Wu et al., 2006). We therefore examined levels of late reverse transcribed products and 2-LTR forms of HIV-1 cDNA in TRIM5α-expressing cells by real time PCR method. Mean C_T values (SD) of late reverse transcribed products were 29.80 (0.27), 29.30 (0.15), and 28.11 (0.10) in cells expressing Rh, AGM, and Hu-R332P TRIM5αs, respectively, while that in control cells was 24.73 (0.08). These results clearly indicated that synthesis of late reverse transcribed products were suppressed in cells expressing functional TRIM5α. When we added MG132, mean C_T values (SD) of late reverse transcribed products were 29.16 (0.13), 28.72 (0.10), and 26.96 (0.15) in cells expressing Rh, AGM, and Hu-R332P TRIM5αs, respectively, and that in control cells was 24.63 (0.11). Differences between C_T values in the presence of MG132 and those in the absence of MG132 were statistically significant ($P<0.05$) in cells expressing Rh, AGM, and Hu-R332P TRIM5αs but not in control cells. We therefore concluded that slight but significant levels of late reverse transcribed products were recovered by MG132 treatment in cells expressing Rh, AGM, and Hu-R332P TRIM5αs. It should be noted that we failed to obtain complete recovery of late reverse transcribed products by MG132 treatment in our experimental system. This was most likely caused by incomplete suppression of proteasome function in our system since SeV-infected MT4 cells could be treated with MG132 for only 2 h to maintain cell viability, while Hela cells were treated with MG132 for 15 h in the previous studies (Anderson et al., 2006; Wu et al., 2006).

With respect to 2-LTR forms of HIV-1 cDNA, mean C_T values (SD) in the absence of MG132 were 39.99 (1.74), 38.32 (2.36), and 37.81 (1.80) in cells expressing Rh, AGM, and Hu-R332P TRIM5αs, respectively, and that in control cells was 33.68 (0.64). In the presence of MG132, mean C_T values (SD) were 40.02 (1.71), 38.71 (1.39), and 36.46 (2.03) in cells expressing Rh, AGM, and Hu-R332P TRIM5αs, respectively, and that in control cells was 33.80 (0.28). Significant recovery of 2-LTR forms of HIV-1 cDNA was thus observed only in cells expressing Hu-R332P TRIM5α ($P<0.05$) but not in cells expressing either AGM or Rh TRIM5αs. These results confirmed that HIV-1 restriction by Rh and AGM TRIM5αs was both proteasome dependent and independent while that by HuR332P TRIM5α was mainly proteasome dependent.

Discussion

Deletion of the RING domain or amino acid changes within the RING domain of Rh TRIM5α has been shown to attenuate anti-HIV-1 activity, but such a mutated TRIM5α still exhibits moderate HIV-1 restriction (Javanbakht et al., 2005; Perez-Caballero et al., 2005b; Stremlau et al., 2004). Both proteasome-dependent and -independent pathways have been proposed in HIV-1 restriction by Rh TRIM5α, since proteasome inhibitor MG132 allows HIV-1 to generate late reverse transcribed products, even though HIV-1 infection and the generation of nuclear 1-LTR and 2-LTR viral cDNA forms remain impaired by Rh TRIM5α (Anderson et al., 2006; Wu et al., 2006). In the study presented here, we demonstrated that the contribution of the RING domain of TRIM5α to retrovirus restriction differed among viral species. SIVmac completely escaped attacks by RING mutants of

Table 1
Summary of TRIM5α-mediated restriction.

	Anti-HIV-1 activity		Anti-SIVmac activity	
TRIM5α	proteasome-dependen	proteasome-independent	proteasome-dependen	proteasome-independent
AGM	yes	yes	yes	no
AGM C15AC18A	no	yes	no	no
AGM with MG132	no	yes	no	no
Hu R332P	yes	no	yes	no
Hu-R332P C15AC18A	no	no	no	no
Hu R332P with MG132	no	no	no	no

Yes, presence of the pathway;
no, absence of the pathway.

Please cite this article as: Maegawa, H., et al., Contribution of RING domain to retrovirus restriction by TRIM5α depends on combination of host and virus, Virology (2010), doi:10.1016/j.virol.2010.01.003

TRIM5α that could still moderately restrict HIV-1 and HIV-2 infection. Addition of proteasome inhibitor MG132 had no effect at all on the anti-HIV-1 activity of AGM TRIM5α, whereas it disrupted at least partly the anti-SIVmac activity of AGM TRIM5α. These results indicate that SIVmac is restricted by AGM TRIM5α mainly in a proteasome-dependent manner, whereas HIV-1 restriction by AGM, Rh, and cynomolgus monkey TRIM5α is both proteasome dependent and independent. In case of Hu-R332P TRIM5α, however, both HIV-1 and SIVmac restrictions were completely eliminated by mutations in the RING domain. Furthermore, both anti-HIV-1 and anti-SIVmac activities of Hu-R332P TRIM5α could also be disrupted by the proteasome inhibitor. These findings indicate that Hu-R332P TRIM5α restricts both HIV-1 and SIVmac mainly via the proteasome-dependent pathway.

It was found that TRIM5α could be poly-ubiquitinated and degraded by the proteasome (Diaz-Griffero et al., 2006). Furthermore, accelerated turnover of TRIM5α was observed during HIV-1 restriction (Rold and Aiken, 2008). Although there is no direct evidence for ubiquitination of the virus core by TRIM5α, it is highly likely that reverse transcription complexes containing viral CA proteins recognized by poly-ubiquitinated TRIM5α would be degraded by the proteasome in combination with TRIM5α. On the other hand, the exact molecular mechanism of the proteasome-independent pathway is still unclear at present. It was previously shown that the incubation of *in vitro* assembled CA proteins composed of recombinant HIV-1 CA–NC fusion proteins with the TRIM5-21R protein containing the Rh TRIM5α B-box, coiled-coil, and SPRY domains and the TRIM21 RING domain caused apparent breaks in the CA structure without any other cellular components (Langelier et al., 2008). It is thus likely that direct binding of Rh TRIM5α proteins to incoming HIV-1 CA proteins causes CA disassembly, which is observed as proteasome-independent restriction. AGM TRIM5α would bind both HIV-1 and SIVmac CA, while it may cause disassembly of the HIV-1 CA but not that of the SIVmac CA. Similarly, Hu-R332P TRIM5α would bind both HIV-1 and SIVmac CA but may fail to cause disassembly of both HIV-1 and SIVmac CAs. We therefore speculate that the proteasome-independent pathway requires specific SPRY–CA interaction that can lead to CA disassembly.

Although the proteasome inhibitor clearly disrupted anti-HIV-1 activity of Hu-R332P and anti-SIVmac activity of AGM, Hu-R332P, and human/AGM TRIM5αs, the number of infected cells never reached the levels of the negative control AGM-TRIM5α-CC(−). Longer exposure of cells expressing the TRIM5αs with the proteasome inhibitor did not increase the number of infected cells (data not shown). In contrast, anti-HIV-1 activity of Hu-R332P and anti-SIVmac activity of AGM and Hu-R332P TRIM5αs were completely eliminated by mutations in the RING domain. The reason for this discrepancy is not clear at present, but it is possible that TRIM5α also exerts a proteasome-independent but RING-dependent restrictive effect.

The RING-proteasome-independent restriction pathway was observed only in anti-HIV-1 but not in anti-SIVmac activity of AGM TRIM5α. It is known that cyclophilin A (CypA) binds to HIV-1 CA via the loop between the 4th and 5th α-helices (L4/5) but not to SIVmac CA (Luban et al., 1993). Since CypA was reported to restrict HIV-1 in monkey cells (Berthoux et al., 2005; Keckesova et al., 2006; Nakayama et al., 2008; Sokolskaja et al., 2006; Stremlau et al., 2006b), it is possible that CypA binding to HIV-1 CA regulates the RING-proteasome-independent restriction mechanism of TRIM5α (Berthoux et al., 2004). This hypothesis prompted us to examine the effect of the RING mutation of TRIM5α on its restrictive effect on NL-ScaVR, an HIV-1 derivative containing SIVmac L4/5 of CA and vif (Kamada et al., 2006). However, NL-ScaVR was similarly restricted by AGM TRIM5α with C15AC18A to HIV-1 (data not shown), indicating that neither the CypA-binding site nor vif is the determining factor in RING-proteasome-independent restriction of HIV-1. Further studies using various chimeric viruses between HIV-1 and SIVmac will also be needed to elucidate the exact molecular mechanisms of the RING-proteasome-independent pathway of TRIM5α mediated HIV-1 restriction.

Conclusion

AGM TRIM5α restricted SIVmac mainly via the proteasome-dependent pathway, whereas HIV-1 and HIV-2 restriction by AGM TRIM5α was both proteasome dependent and independent. In contrast, Hu-R332P restricts both HIV-1 and SIVmac mainly via the proteasome-dependent pathway. We concluded that the mechanisms of retrovirus restriction by TRIM5α vary depending on the combination of host and virus.

Materials and methods

Plasmid construction and protein expression

Previous reports have described recombinant Sendai viruses (SeVs) expressing C-terminally HA-tagged AGM TRIM5α (GenBank accession number AB210050), Rh TRIM5α (GenBank accession number AY625001), cynomolgus monkey (CM) TRIM5α (GenBank accession number AB210052), human TRIM5α (This human TRIM5α cDNA was obtained from T cell line MT4 and there was a single glycine-to-aspartic acid substitution at an amino acid position 249 compared with GenBank accession number NM033034.1), human TRIM5α with R332P, human and AGM chimeric TRIM5α and AGM TRIM5α lacking the coiled-coil domain (AGM-TRIM5α-CC(−)) (Kono et al., 2008; Maegawa et al., 2008; Nakayama et al., 2005, 2007). In the present study, a PCR-based mutagenesis was used to generate cDNA of the following C-terminally HA-tagged AGM TRIM5α RING domain mutants: AGM TRIM5α with C15AC18A, AGM TRIM5α with C30AH32A, AGM TRIM5α with C15AC18A-C30AH32A, and human TRIM5α with R332P and C15AC18A mutations. The entire coding sequences of those TRIM5αs were then transferred to the NotI site of pSeV18+b(+). Recombinant SeVs expressing various TRIM5αs were obtained with a previously described method (Shioda et al., 2001).

The plasmid expressing myc-tagged ubiquitin (myc-Ub) was generated according to the previous publication (Ellison and Hochstrasser, 1991). Briefly, human ubiquitin cDNA (NM_018955) was amplified by reverse transcription-PCR from the human epithelial carcinoma cell line HeLa by using 5′-GCGAATGCCATGACTGAAG-3′ and 5′-GACGTGGTTGGTGATTGGC-3′ followed by nested PCR using 5′-ATGCAGATCTTCGTGAAAACC-3′ and 5′-CTAACCACCTCTCAGACGCAG-GACC-3′. The amplified products were then cloned into pCR-2.1 TOPO (Invitrogen, Carlsbad, CA). The entire coding sequences of the myc-Ub were then transferred to the NheI and NotI site of pcDNA3.1(-) (Invitrogen, Carlsbad, CA).

Immunoprecipitation and Western blot analysis

For protein expression analysis, human T-cell line MT4 was infected with SeV at a multiplicity of infection (MOI) of 10 plaque forming units (PFU) per cell, and incubated at 37 °C for 16 h. The cells were then lysed in RIPA buffer (10 mM Tris–HCl (pH 7.4) containing 100 mM NaCl, 1% Sodium deoxycholate, and 0.1% sodium dodecyl sulfate), and the cell lysates were subjected to sodium dodecyl sulfate-polyacrylamide gel electrophoresis (SDS-PAGE). Proteins in the gel were transferred to a membrane (Immobilon; Millipore, Billerica, MA), and blots were blocked and probed with an anti-HA High Affinity rat monoclonal antibody (Roche, Indianapolis, IN) overnight at 4 °C. Blots were then incubated with peroxidase-conjugated anti-rat IgG (American Qualex, San Clemente, CA). Bound antibodies were visualized with ChemiLumi-One L chemiluminescent kit (Nacalai Tesque, Kyoto, Japan).

Please cite this article as: Maegawa, H., et al., Contribution of RING domain to retrovirus restriction by TRIM5α depends on combination of host and virus, Virology (2010), doi:10.1016/j.virol.2010.01.003

For ubiquitination analysis, the NotI and EcoRI sites were used to construct the plasmid expressing HA-tagged TRIM5α RING mutants in pcDNA3.1(-). DMRIE-C reagent (Invitrogen, Carlsbad, CA) was used to transfect 293 T cells with 1 μg of plasmid encoding HA-tagged wild-type or mutant TRIM5αs together with 1 μg of plasmid expressing myc-Ub in six-well plates. Forty-eight hours later, the cells were lysed and TRIM5α proteins in the lysates were precipitated with a Protein G-immunoprecipitation kit (Roche, Indianapolis, IN) using the anti-HA rat monoclonal antibody. After overnight incubation at 4 °C, beads were washed three times in RIPA buffer. Precipitated proteins were detected with the same procedure as above except that an anti-myc mouse monoclonal antibody and peroxidase-conjugated anti-mouse IgG (Kirkegaard and Perry Laboratories, Gaithersburg, MD) were used for visualizing the myc-tagged Ub protein.

Virus preparation

HIV-1-NL43, HIV-2 GH123 or SIVmac239 was prepared by transfection of 293 T cells with pNL432 (Adachi et al., 1986), pGH123 (Shibata et al., 1990), or pBRmac239 (Kastler et al., 1991), respectively. The vesicular stomatitis virus glycoprotein (VSV-G) pseudotyped HIV-1 vector expressing green fluorescence protein (GFP) (HIV-1-GFP) was prepared as described previously (Miyoshi et al., 1997, 1998) as was VSV-G pseudotyped SIVmac vector expressing GFP (SIVmac-GFP) (Hofmann et al., 1999). The viral titer was determined by measuring viral CA protein, p24, p25 or p27, with a RetroTek antigen ELISA kit (ZeptoMetrix, Buffalo, NY).

Viral infection

MT4 or canine Cf2Th cells were infected with SeV expressing various TRIM5αs. Nine hours after SeV infection, 1.0×10^5 cells per dose were superinfected with serially diluted HIV-1-GFPs or SIVmac-GFPs in 48-well plates and incubated at 37 °C. Forty hours after infection, the infected cells were fixed with 1% formaldehyde and counted with a flow cytometer (FACScaliber; Becton Dickinson, Franklin Lakes, NJ). For the HIV-1, HIV-2 or SIVmac replication assay, 2.0×10^5 MT4 cells were infected with SeV expressing various TRIM5αs and 9 h after SeV infection, the cells were superinfected with 20 ng of p24 of HIV-1 NL43, p25 of HIV-2 GH123 or p27 of SIVmac. The culture supernatants were collected periodically for measurement of the p24, p25 or p27 levels.

Proteasome inhibition and infection with HIV-1-GFP or SIVmac-GFP

MT4 cells were infected with SeV expressing various TRIM5αs. Nine hours after SeV infection, 1.0×10^5 cells were superinfected with 10 ng of p24 of HIV-1-GFP or 100 ng of p27 of SIVmac-GFP in the presence of 10 μM MG132 (CALBIOCHEM) in 0.1% DMSO or 0.1% DMSO only. Two hours after the HIV-1-GFP or SIVmac-GFP infection, the cells were washed in fresh medium and incubated at 37 °C for 40 h. The infected cells were fixed with 1% formaldehyde and then counted with a flow cytometer.

Immunofluorescence confocal microscopy

AGM CV1 cells infected with SeV expressing several TRIM5αs at an MOI of 10 PFU per cell were fixed 24 h after infection in 3% paraformaldehyde in PBS, permeabilized with 0.05% saponin and 0.2% bovine serum albumin in PBS, and incubated with the anti-HA rat monoclonal antibody. Bound antibodies were then detected with a FITC-conjugated goat antibody directed against rat IgG (American Qualex Antibodies, San Clemente, CA). Indirect immunofluorescence was visualized with a Radiance 2000 laser confocal microscope system (Bio-Rad Laboratories, Hercules, CA).

Real-time PCR analysis

To prepare high titer virus stock of HIV-1 NL43, MT4 cells were infected with NL43 virus and the culture supernatant was harvested at its peak titer (1250 ng/ml of p24) at 12 days after infection. Five x 10^6 MT4 cells were infected with SeV expressing TRIM5α. Twenty hours after SeV infection, cells were superinfected with 500 μl (625 ng of p24) of NL43 stock virus with 10 μM MG132 (CALBIOCHEM) in 0.1% DMSO or with 0.1% DMSO only for 2 h. After washing out of inoculated virus containing MG132, cells were suspended in 10 ml of flesh media and incubated at 37 C for 12 h. Total DNA was extracted by using QIAamp DNA Blood kit. Real-time PCR was performed with an Applied Biosystems 7500 Real-Time PCR System to analyze viral cDNA synthesis. Primers and Taqman probes for late reverse transcribed products and 2-LTR forms were designed according to Julias et al. (2001) and Van Maele et al. (2003), and 0.6 μg DNA were subjected to 40 cycles of PCR in 10 μl reaction mixture. Threshold cycle (C_T) values were calculated by 7500 Fast System SDS software (Applied Biosystems). Mean C_T values and their standard deviation (SD) were calculated in triplicate (late reverse transcribed product) or septuplicate (2-LTR) samples. In a few cases we failed to detect amplification of 2-LTR forms, the C_T values were assigned as 41 cycles. Statistical significance of observed difference in mean C_T values was evaluated by Mann-Whitney *U* test.

Uncited references Q2

Berthous et al., 2004
Kestler et al., 1991

Acknowledgements

We are grateful to J. Sodroski and F. Diaz-Griffero (Harvard Medical School, Boston, USA) for providing the pSIvec1.GFP plasmid. We also wish to thank S. Sakuragi for her helpful discussions and S. Bando and N. Teramoto for their assistance. This work was supported by grants from the Ministry of Education, Culture, Sports, Science, and Technology, the Ministry of Health, Labor and Welfare, and the Health Science Foundation of Japan.

References

Abe, H., Miyamoto, K., Tochio, N., Koshiba, S., Kigawa, T., Yokoyama, S., 2007. Solution structure of the zinc finger, C3hc4 type (ring finger) domain of tripartite motif-containing protein 5. MMDB: Entrez's 3D-structure database. MMDB ID: 62462. http://www.ncbi.nlm.nih.gov/Structure/mmdb/mmdbsrv.cgi?Dopt = s&uid = 62462

Adachi, A., Gendelman, H.E., Koenig, S., Folks, T., Willey, R., Rabson, A., Martin, M.A., 1986. Production of acquired immunodeficiency syndrome associated retrovirus in human and nonhuman cells transfected with an infectious molecular clone. J. Virol. 59, 284–291.

Anderson, J.L., Campbell, E.M., Wu, X., Vandegraaff, N., Engelman, A., Hope, T.J., 2006. Proteasome inhibition reveals that a functional preintegration complex intermediate can be generated during restriction by diverse TRIM5 proteins. J. Virol. 80, 9754–9760.

Berthous, L., Sebastian, S., Sokolskaja, E., Luban, J., 2004. Lv1 inhibition of human immunodeficiency virus type 1 is counteracted by factors that stimulate synthesis or nuclear translocation of viral cDNA. J. Virol. 78, 11359–11739.

Berthoux, L., Sebastian, S., Sokolskaja, E., Luban, J., 2005. Cyclophilin A is required for TRIM5α-mediated resistance to HIV-1 in Old World monkey cells. Proc. Natl. Acad. Sci. U.S.A. 102, 14849–14853.

Borden, K.L., Boddy, M.N., Lally, J., O'Reilly, N.J., Martin, S., Howe, K., Solomon, E., Freemont, P.S., 1995. The solution structure of the RING finger domain from the acute promyelocytic leukaemia proto-oncoprotein PML. EMBO J. 14, 1532–1541.

Borden, K.L., Freemont, P.S., 1996. The RING domain: a recent example of a sequence-structure family. Curr. Opin. Struct. Biol. 1996 (6), 395–401.

Diaz-Griffero, F., Li, X., Javanbakht, H., Song, B., Welikala, S., Stremlau, M., Sodroski, J., 2006. Rapid turnover and polyubiquitylation of the retroviral restriction factor TRIM5. Virology 349, 300–315.

Ellison, M.J., Hochstrasser, M., 1991. Epitope-tagged ubiquitin. A new probe for analyzing ubiquitin function. J. Biol. Chem. 266, 21150–21157.

Gao, F., Bailes, E., Robertson, D.L., Chen, Y., Rodenburg, C.M., Michael, S.F., Cummins, L.B., Arthur, L.O., Peeters, M., Shaw, G.M., Sharp, P.M., Hahn, B.H., 1999. Origin of HIV-1 in the chimpanzee Pan troglodytes troglodytes. Nature 397, 436–441.

Please cite this article as: Maegawa, H., et al., Contribution of RING domain to retrovirus restriction by TRIM5α depends on combination of host and virus, Virology (2010), doi:10.1016/j.virol.2010.01.003

Hofmann, W., Schubert, D., LaBonte, J., Munson, L., Gibson, S., Scammell, J., Ferrigno, P., Sodroski, J., 1999. Species-specific, postentry barriers to primate immunodeficiency virus infection. J. Virol. 73, 10020–10028.

Jackson, P.K., Eldridge, A.G., Freed, E., Furstenthal, L., Hsu, J.Y., Kaiser, B.K., Reimann, J.D., 2000. The role of the RINGs: substrate recognition and catalysis by ubiquitin ligases. Trends Cell Biol. 10, 429–439.

Javanbakht, H., Diaz-Griffero, F., Stremlau, M., Si, Z., Sodroski, J., 2005. The contribution of RING and B-box 2 domains to retrovirus restriction mediated by monkey TRIM5α. J. Biol. Chem. 280, 26933–26940.

Javanbakht, H., Yuan, W., Yeung, D.F., Song, B., Diaz-Griffero, F., Li, Y., Li, X., Stremlau, M., Sodroski, J., 2006. Characterization of TRIM5α trimerization and its contribution to human immunodeficiency virus capsid binding. Virology 353, 234–246.

Julias, J.G., Ferris, A.L., Boyer, P.L., Hughes, S.H., 2001. Replication of phenotypically mixed human immunodeficiency virus type 1 virions containing catalytically active and catalytically inactive reverse transcriptase. J. Virol. 6537–6546.

Kamada, K., Igarashi, T., Martin, M.A., Khamsri, B., Hatcho, K., Yamashita, T., Fujita, M., Uchiyama, T., Adachi, A., 2006. Generation of HIV-1 derivatives that productively infect macaque monkey lymphoid cells. Proc. Natl. Acad. Sci. U.S.A. 103, 16959–16964.

Keckesova, Z., Ylinen, L.M., Towers, G.J., 2006. Cyclophilin A renders human immunodeficiency virus type 1 sensitive to old world monkey but not human TRIM5α antiviral activity. J. Virol. 80, 4683–4690.

Kestler III, H.W., Ringler, D.J., Mori, K., Panicali, D.L., Sehgal, P.K., Daniel, M.D., Desrosiers, R.C., 1991. Importance of the nef gene for maintenance of high virus loads and for development of AIDS. Cell 65, 651–662.

Kono, K., Song, H., Shingai, Y., Shioda, T., Nakayama, E.E., 2008. Comparison of anti-viral activity of rhesus monkey and cynomolgus monkey TRIM5αs against HIV-2 infection. Virology 373, 447–456.

Langelier, C.R., Sandrin, V., Eckert, D.M., Christensen, D.E., Chandrasekaran, V., Alam, S.L., Aiken, C., Olsen, J.C., Kar, A.K., Sodroski, J.G., Sundquist, W.I., 2008. Biochemical characterization of a recombinant TRIM5α protein that restricts human immunodeficiency virus type 1 replication. J. Virol. 82, 11682–11694.

Luban, J., Bossolt, K.L., Franke, E.K., Kalpana, G.V., Goff, S.P., 1993. Human immunodeficiency virus type 1 Gag protein binds to cyclophilins A and B. Cell 73, 1067–1078.

Maegawa, H., Nakayama, E.E., Kuroishi, A., Shioda, T., 2008. Silencing of tripartite motif protein (TRIM) 5α mediated anti-HIV-1 activity by truncated mutant of TRIM5α. J. Virol. Methods 151, 249–256.

Mische, C.C., Javanbakht, H., Song, B., Diaz-Griffero, F., Stremlau, M., Strack, B., Si, Z., Sodroski, J., 2005. Retroviral restriction factor TRIM5α is a trimer. J. Virol. 79, 14446–14450.

Miyoshi, H., Takahashi, M., Gage, F.H., Verma, I.M., 1997. Stable and efficient gene transfer into the retina using an HIV-based lentiviral vector. Proc. Natl. Acad. Sci. U.S.A. 94, 10319–10323.

Miyoshi, H., Blomer, U., Takahashi, M., Gage, F.H., Verma, I.M., 1998. Development of a self-inactivating lentivirus vector. J. Virol. 72, 8150–8157.

Nakayama, E.E., Miyoshi, H., Nagai, Y., Shioda, T., 2005. A specific region of 37 amino acid residues in the SPRY (B30.2) domain of African green monkey TRIM5α determines species-specific restriction of simian immunodeficiency virus SIVmac infection. J. Virol. 79, 8870–8877.

Nakayama, E.E., Carpentier, W., Costagliola, D., Shioda, T., Iwamoto, A., Debre, P., Yoshimura, K., Autran, B., Matsushita, S., Theodorou, I., 2007. Wild type and H43Y variant of human TRIM5α show similar anti-human immunodeficiency virus type 1 activity both in vivo and in vitro. Immunogenetics 59, 511–515.

Nakayama, E.E., Shingai, Y., Kono, K., Shioda, T., 2008. TRIM5α-independent anti-human immunodeficiency virus type 1 activity mediated by cyclophilin A in Old World monkey cells. Virology 375, 514–520.

Perez-Caballero, D., Hatziioannou, T., Yang, A., Cowan, S., Bieniarz, P.D., 2005a. Human tripartite motif 5α domains responsible for retrovirus restriction activity and specificity. J. Virol. 79, 8969–8978.

Perez-Caballero, D., Hatziioannou, T., Zhang, F., Cowan, S., Bieniasz, P.D., 2005b. Restriction of human immunodeficiency virus type 1 by TRIM-CypA occurs with rapid kinetics and independently of cytoplasmic bodies, ubiquitin, and proteasome activity. J. Virol. 79, 15567–15572.

Reymond, A., Meroni, G., Fantozzi, A., Merla, G., Cairo, S., Luzi, L., Riganelli, D., Zanaria, E., Messali, S., Cainarca, S., Guffanti, A., Minucci, S., Pelicci, P.G., Ballabio, A, 2001. The tripartite motif family identifies cell compartments. EMBO J. 20, 2140–2151.

Rold, C.J., Aiken, C., 2008. Proteasomal degradation of TRIM5α during retrovirus restriction. PLoS. Pathog. 4, 5.

Sawyer, S.L., Wu, L.I., Emerman, M., Malik, H.S., 2005. Positive selection of primate TRIM5α identifies a critical species-specific retrovirus restriction domain. Proc. Natl. Acad. Sci. U.S.A. 102, 2832–2837.

Sawyer, S.L., Emerman, M., Malik, H.S., 2007. Discordant evolution of the adjacent antiretroviral gnens *TRIM22* and *TRIM5* in mammals. PloS Pathog. 3, 1918–1929.

Sebastian, S., Luban, J., 2005. TRIM5alpha selectively binds a restriction-sensitive retroviral capsid. Retrovirology 2, 40.

Shibata, R., Miura, T., Hayami, M., Ogawa, K., Sakai, H., Kiyomasu, T., Ishimoto, A., Adachi, A., 1990. Mutational analysis of the human immunodeficiency virus type 2 (HIV-2) genome in relation to HIV-1 and simian immunodeficiency virus SIV (AGM). J. Virol. 64, 742–747.

Shioda, T., Nakayama, E.E., Tanaka, Y., Xin, X., Liu, H., Kawana-Tachikawa, A., Kato, A., Sakai, Y., Nagai, Y., Iwamoto, A., 2001. Naturally occurring deletional mutation in the C-terminal cytoplasmic tail of CCR5 affects surface trafficking of CCR5. J. Virol. 75, 3462–3468.

Sokolskaja, E., Berthoux, L., Luban, J., 2006. Cyclophilin A and TRIM5α independently regulate human immunodeficiency virus type 1 infectivity in human cells. J. Virol. 80, 2855–2862.

Song, B., Javanbakht, H., Perron, M., Park, D.H., Stremlau, M., Sodroski, J., 2005. Retrovirus restriction by TRIM5α variants from Old World and New World Primates. J. Virol. 79, 3930–3937.

Stremlau, M., Owens, C.M., Perron, M.J., Kiessling, M., Autissier, P., Sodroski, J., 2004. The cytoplasmic body component TRIM5α restricts HIV-1 infection in Old World monkeys. Nature 427, 848–853.

Stremlau, M., Perron, M., Welikala, S., Sodroski, J., 2005. Species-specific variation in the B30.2 (SPRY) domain of TRIM5α determines the potency of human immunodeficiency virus restriction. J. Virol. 79, 3139–3145.

Stremlau, M., Perron, M., Lee, M., Li, Y., Song, B., Javanbakht, H., Diaz-Griffero, F., Anderson, D.J., Sundquist, W.I., Sodroski, J., 2006a. Specific recognition and accelerated uncoating of retroviral capsids by the TRIM5α restriction factor. Proc. Natl. Acad. Sci. U.S.A. 103, 5514–5519.

Stremlau, M., Song, B., Javanbakht, H., Perron, M., Sodroski, J., 2006b. Cyclophilin A: an auxiliary but not necessary cofactor for TRIM5α restriction of HIV-1. Virology 351, 112–120.

Van Maele, B., Rijck, J.D., Clercq, E.D., Debyser, Z., 2003. Impact of the central polypurine tract on the kinetics of human immunodeficiency virus type 1 vector transduction. J. Virol. 4685–4694.

Wu, X., Anderson, J.L., Campbell, E.M., Joseph, A.M., Hope, T.J., 2006. Proteasome inhibitors uncouple rhesus TRIM5α restriction of HIV-1 reverse transcription and infection. Proc. Natl. Acad. Sci. U.S.A. 103, 7465–7470.

Yap, M.W., Nisole, S., Stoye, J.P., 2005. A single amino acid change in the SPRY domain of human TRIM5α leads to HIV-1 restriction. Curr. Biol. 15, 73–78.

Please cite this article as: Maegawa, H., et al., Contribution of RING domain to retrovirus restriction by TRIM5α depends on combination of host and virus, Virology (2010), doi:10.1016/j.virol.2010.01.003

JOURNAL OF VIROLOGY, Apr. 2007, p. 3757–3768 Vol. 81, No. 8
0022-538X/07/$08.00+0 doi:10.1128/JVI.01544-06

Impact of V2 Mutations on Escape from a Potent Neutralizing Anti-V3 Monoclonal Antibody during In Vitro Selection of a Primary Human Immunodeficiency Virus Type 1 Isolate[▽]

Junji Shibata,[1] Kazuhisa Yoshimura,[1] Akiko Honda,[1] Atsushi Koito,[1] Toshio Murakami,[2] and Shuzo Matsushita[1]*

Division of Clinical Retrovirology and Infectious Diseases, Center for AIDS Research, Kumamoto University, Kumamoto 860-0811,[1] and The Chemo-Sero-Therapeutic Research Institute, Kyokushi, Kikuchi, Kumamoto 869-1298,[2] Japan

Received 19 July 2006/Accepted 16 January 2007

KD-247, a humanized monoclonal antibody to an epitope of gp120-V3 tip, has potent cross-neutralizing activity against subtype B primary human immunodeficiency virus type 1 (HIV-1) isolates. To assess how KD-247 escape mutants can be generated, we induced escape variants by exposing bulked primary R5 virus, MOKW, to increasing concentrations of KD-247 in vitro. In the presence of relatively low concentrations of KD-247, viruses with two amino acid mutations (R166K/D167N) in V2 expanded, and under high KD-247 pressure, a V3 tip substitution (P313L) emerged in addition to the V2 mutations. However, a virus with a V2 175P mutation dominated during passaging in the absence of KD-247. Using domain swapping analysis, we demonstrated that the V2 mutations and the P313L mutation in V3 contribute to partial and complete resistance phenotypes against KD-247, respectively. To identify the V2 mutation responsible for the resistance to KD-247, we constructed pseudoviruses with single or double amino acid mutations in V2 and measured their sensitivity to neutralization. Interestingly, the neutralization phenotypes were switched, so that amino acid residue 175 (Pro or Leu) located in the center of V2 was exchanged, indicating that the amino acid at position 175 has a crucial role, dramatically changing the Env oligomeric state on the membrane surface and affecting the neutralization phenotype against not only anti-V3 antibody but also recombinant soluble CD4. These data suggested that HIV-1 can escape from anti-V3 antibody attack by changing the conformation of the functional envelope oligomer by acquiring mutations in the V2 region in environments with relatively low antibody concentrations.

The envelope protein (Env) of human immunodeficiency virus type 1 (HIV-1) presents on the virus surface as "spikes" composed of trimers comprising three gp120-gp41 complexes (6, 32, 33). Among the regions that induce the neutralization antibody (NAb) response, the third variable domain (V3 loop) of gp120 is considered one of the major targets of the host immune response (23, 69). It has been estimated that as much as half of the antibody response against HIV-1 Env in patient serum is directed against the V3 region (43). A recent crystallographic study revealed that the V3 loop contains features that are essential for coreceptor binding and that the extended nature and antibody accessibility of V3 are associated with its immunodominance (20).

HIV-1 primary isolates are relatively resistant to neutralization by NAbs and recombinant soluble CD4 (rsCD4) compared with variants selected for growth in permanent cell lines (42, 52, 55). Studies addressing differences between neutralization-sensitive and -resistant variants have revealed the involvement of several mechanisms that underlie the neutralization resistance of primary isolates, including the occlusion of epitopes within the oligomer, extensive glycosylation, and extension of variable loops from the surface of the complex, as well as steric and conformational blocking of receptor binding sites (7, 12, 32, 38, 49, 50, 54, 62). The structural features of gp120 tolerate a vast array of mutations that permit the selection of neutralization escape variants, as has been previously demonstrated in culture assays, animal models, and infected individuals (24).

Although there are ample data showing that NAbs can protect against HIV-1 infection in vitro and in animal models in vivo, activity in infected humans remains controversial (3, 4, 9, 14, 22, 40, 48, 58). Studies addressing NAbs in primary infections have suggested that most recently infected individuals mount a vigorous antibody response against autologous viruses. However, the rapid evolution of HIV in the presence of NAbs results in the emergence of escape mutants. As a consequence, at any time during an early stage of the HIV disease, NAbs are more likely to recognize earlier autologous viruses than contemporaneous ones. Despite evidence of phenotypic resistance, the genetic basis of the mechanism allowing primary viruses to escape from NAbs is poorly understood. Wei et al. found that glycosylation in the envelope plays an important role in allowing escape from neutralization (62). In contrast, in a recent study Frost et al. found that viral escape from NAbs is correlated with the rate of amino acid substitution rather than changes in glycosylation or insertions or deletions in the envelope (14). Because of the polyclonal nature of NAbs in patient sera, it is difficult to clarify the genetic mechanism responsible for neutralization escape.

* Corresponding author. Mailing address: Division of Clinical Retrovirology and Infectious Diseases, Center for AIDS Research, Kumamoto University, Kumamoto 860-0811, Japan. Phone: 81 96 373 6536. Fax: 81 96 373 6537. E-mail: shuzo@kaiju.medic.kumamoto-u.ac.jp.

▽ Published ahead of print on 24 January 2007.

Neutralization escape from anti-V3 monoclonal antibodies (MAbs) has been induced in T-cell-line-adapted viruses in several experiments and associated with amino acid substitution within the epitope in the V3 loop (8, 37, 65). However, Park et al. showed that human sera with neutralizing antibodies that contained polyclonal antibodies directed at the V3 region induced neutralization-resistant variants without V3 amino acid substitution (46). Neutralization studies using anti-V3 antibodies against primary isolates suggest that the neutralization resistance phenotype is associated with changes in the sequences outside V3, rather than variation within the V3 epitope (29, 62). However, the contribution of each change in the envelope to the emergence of escape mutants remains unclear because they are not selected under neutralizing MAb pressure.

Recently, we described a humanized MAb, KD-247, that displayed cross-neutralizing activity against HIV-1 clade B isolates (11). The epitope of KD-247 was mapped to six amino acids around the PGR core sequence at the tip of the V3 loop. The shortest reactive peptide recognized by KD-247 was determined to be IGPGR, which is shared by 49% of HIV-1 isolates in clade B (35). In addition, complete protection from challenge infection by a pathogenic strain of simian-human immunodeficiency virus 89.6 was observed when a high concentration of the antibody was used in an animal model (10). A molecularly cloned CCR5-tropic HIV-1 strain, JR-FL, which is relatively resistant to neutralization (15, 50), was exposed to KD-247 to obtain a neutralization escape mutant (67). Induction of the neutralization-resistant virus with a mutation in the V3 tip was observed in the presence of a high concentration of KD-247, and the escape variant was found to be more sensitive to CCR5 inhibitors and rsCD4 than the original strain (67).

The present study sought to understand how virus mutation impacts the activity of an anti-V3 MAb, KD-247. For this we subjected a primary R5 virus, MOKW, to selection pressure by KD-247. The present data suggested that it is necessary to pass a phased step so that the escape mutant against the anti-V3 antibody can emerge. Neutralization escape variants with V2 mutations in gp120 could be selected at relatively low KD-247 pressures, but high concentrations of KD-247 were required for induction of a completely resistant variant with amino acid substitution in the epitope. Moreover, we present evidence suggesting that some V2 mutations change the tertiary or quaternary structure of the envelope trimers on the viral surface that are involved in the neutralization resistance of the primary isolate. Clarification of the mechanisms responsible for this neutralization resistance may provide important insight into possible methods for the induction of potent and cross-neutralizing antibody responses capable of neutralizing various primary isolates.

(This work was presented in part at the 13th Conference on Retroviruses and Opportunistic Infection, Denver, CO, 5 to 8 February 2006 [55a].)

MATERIALS AND METHODS

Cells, culture conditions, reagents, and viruses. PM1/CCR5 cells (68) were maintained in RPMI 1640 medium (Sigma) supplemented with 10% heat-inactivated fetal calf serum (FCS; HyClone Laboratories, Logan, UT), 50 U/ml of penicillin, 50 mg/ml of streptomycin, and 100 μg/ml of G418 (Sigma). 293T cells were maintained in Dulbecco's modified Eagle medium (Sigma) supplemented with 10% heat-inactivated FCS. The CD4- and CCR5-expressing human osteogenic sarcoma cell line GHOST-hi5 was maintained in Dulbecco's modified Eagle medium supplemented with 10% FCS, G418 (200 μg/ml), hygromycin B (100 μg/ml; Sigma), and puromycin (1 μg/ml; Sigma).

KD-247, an anti-gp120-V3 antibody, was produced as previously described (11). 17b, a monoclonal antibody against the CD4-induced epitope, and immunoglobulin Gb12 (IgGb12), a monoclonal antibody against the CD4-binding epitope, were provided by the National Institutes of Health AIDS Research and Reference Reagent Program. 447-52D, an anti-gp120 V3 MAb, was a gift from Suzan Zolla-Pazner (New York University School of Medicine). 2D7, an anti-CCR5 MAb, and RPA-T4, an anti-CD4 MAb, were purchased from BD Biosciences Pharmingen (San Jose, CA). Human rsCD4 was purchased from R&D Systems, Inc. (Minneapolis, MN). TAK-779, a CCR5 inhibitor, was kindly provided by Takeda Chemical Industries, Ltd. (Osaka, Japan). AK-602, a CCR5 inhibitor, was gifted by Ono Pharmaceutical Co., Ltd. (Osaka, Japan).

The R5 primary HIV-1, MOKW virus, was isolated from a drug-naïve Japanese patient (36). This virus was passaged in phytohemagglutinin-activated peripheral blood mononuclear cells (PBMCs), and the culture supernatant was stored at −80°C until use.

Isolation of a KD-247-resistant mutant from MOKW virus in vitro. The selection of KD-247 escape variants from MOKW virus was performed as previously described (67). Briefly, MOKW virus was preincubated in the presence of KD-247 for 30 min at 37°C, and then PM1/CCR5 cells (4×10^4) were exposed to 500 times the 50% tissue culture infective dose ($TCID_{50}$) of the preincubated MOKW. After incubation for 5 h at 37°C, cells were pelleted down and resuspended in RPMI 1640 medium supplemented with 10% FCS without KD-247. Viral replication was monitored by observation of the cytopathic effects in PM1/CCR5 cells. The culture supernatant was harvested on day 7 and used to infect fresh PM1/CCR5 cells for the next round of culture in the presence of increasing concentrations of KD-247. When the virus began to propagate rapidly in the presence of KD-247, the MAb concentration was further increased. After the virus was passaged in the presence of up to 2,000 μg/ml KD-247 in PM1/CCR5 cells, a KD-247-resistant virus, MOKW9p(2000), was recovered from the cell culture supernatant. MOKW virus was also passaged for the same time period in PM1/CCR5 cells in the absence of KD-247, and the resulting virus was designated MOKW9p(−).

Amplification of viral cDNA and nucleotide sequencing. Viral RNA was extracted from cell culture supernatants with several concentrations of KD-247 using a QIAamp viral RNA kit (QIAGEN). Viral RNAs were reverse transcribed using a High Capacity cDNA Archive Kit (Applied Biosystems) with specific antisense primer ENVN (5′-CTGCCAATCAGGGAAGTAGCCTTGT GT-3′). Nested PCR was performed to amplify the gp120 C1 to C4 coding region as described previously (60). The primers used were as follows: for the first-step PCR, 1B (5′-AGAAAGAGCAGAAGACAGTGGCAATGA-3′) and H (5′-TA GTGCTTCCTGCTGCTCCCAAGAACCC-3′); for the second-step PCR, 2B (5′-AGCAGAAGACAGTGGCAATGAGAGTGA-3′) and F (5′-ATATAATT CACTTCTCCAATTGTCCCTCAT-3′). The products of the nested PCR were inserted in the TA vector (Invitrogen) and sequenced using a Big Dye Terminator, version 1.1 (Applied Biosystems), in accordance with the manufacturer's instructions.

MTT assay. The neutralization-sensitivities of each passaged MOKW virus to KD-247 were determined as previously described (67). Briefly, PM1/CCR5 cells (2×10^3 cells/well) were exposed to 100 $TCID_{50}$ of each passaged virus in the presence of various concentrations of KD-247 in 96-well round-bottom microculture plates and incubated at 37°C for 7 days. After removal of 100 μl of medium from each well, 10 μl of MTT (3-[4,5-dimethylthiazol-2-yl]-2,5-diphenyl tetrazolium bromide) solution (7.5 mg/ml) in phosphate-buffered saline (PBS) was added to each well, and the plate was incubated at 37°C for 3 h. After incubation, 100 μl of acidified isopropanol containing 4% (vol/vol) Triton X-100 was added to each well to dissolve the formazan crystals. The optical density (wavelength, 570 nm) was measured using a microplate reader. Assays were performed in duplicate or triplicate.

Construction of mutant envelope expression vectors. Proviral DNA was extracted from each batch of passaged MOKW virus-infected PM1/CCR5 cells using a QIAamp DNA blood mini kit (QIAGEN). For the construction of each passaged envelope expression vector, we used pCXN2, which has a chicken actin promoter. Briefly, we amplified MOKW gp160 regions using LA *Taq* (Takara) with primers ENVA (5′-GGCTTAGGCATCTCCTATGGCAGGAAGAA-3′) and ENVN (see above). The products of the PCR were inserted into pCR-XL-TOPO (Invitrogen). The sequences of the amplified *env* region of MOKW virus were confirmed using an ABI377 automated DNA sequencer. The EcoRI fragment of pCR-XL-MOKW containing the entire *env* region was ligated into pCXN2 to give pCXN-MOKW-RDP (the last three letters of the MOKW virus

constructs represent the amino acids at positions 166, 167, and 175 in the V2 region), pCXN-MOKW-KNL/C3m, and pCXN-MOKW-KNL/V3m. The pCXN-MOKW-KNL vector was constructed by replacing the StuI-Bsu36I fragment of pCXN-MOKW-KNL/C3m with a corresponding MOKW-RDP fragment. The pCXN-MOKW-RDP/V3m and pCXN-MOKW-RDP/C3m vectors were constructed by replacing the StuI-Bsu36I fragment of pCXN-MOKW-RDP with the corresponding pCXN-MOKW-KNL/V3m or pCXN-MOKW-KNL/C3m fragments, respectively. pCXN-MOKW-KNP, pCXN-MOKW-RDL, pCXN-MOKW-KDL, and pCXN-MOKW-RNL were generated by site-directed mutagenesis using a QuickChange Site-Directed Mutagenesis Kit (Stratagene) in accordance with the manufacturer's instructions.

Pseudovirus preparation. Five micrograms of pNL4-3.luc.R$^-$E$^-$ and 0.5 μg of pRSV-Rev (18), supplied by the NIH AIDS Research and Reference Reagent Program, and 4.5 μg of the MOKW Env-expressing pCXN2 were cotransfected into 293T cells using Effectene transfection reagent (QIAGEN). At 24 h after the transfection, the pseudovirus-containing supernatants were harvested, filtered through a 0.2-μm-pore-size filter, and stored at −80°C. To measure the pseudovirus activity, a luminescence assay using GHOST-hi5 cells was used as previously described (60).

Neutralization assays. A single-cycle infectivity assay was used to measure the neutralization of MOKW pseudoviruses as described previously (60). Briefly, MAbs at various concentrations and a pseudovirus suspension corresponding to 100 $TCID_{50}$ were preincubated on ice for 15 min. The virus-antibody mixtures were added to GHOST-hi5 cells, which on the preceding day had been seeded in a 96-well plate (1.5×10^4 cells/well). Cultures were incubated for 2 days at 37°C, washed with PBS, and lysed with lysis buffer (Luc PGC-50; PicaGene). Following transfer of the cell lysates to luminometer plates (Coastar 3912), the luciferase activity (in relative light units) in each well was measured using luciferase substrate (100 μl/well; PicaGene) in a TR717 microplate luminometer (Applied Biosystems). The reduction in infectivity was determined by comparing the relative light units in the presence and absence of MAbs and was expressed as the percentage of neutralization. The same assay was repeated two to three times.

In vitro binding assay to the MOKW envelope-expressing cell surfaces. In vitro binding assays were performed as previously described (53, 67). EcoRI fragments of MOKW *env* genes from pXL-MOKWs were subcloned into the corresponding sites in pDNR-1r (Clontech). The vectors were sequenced to confirm the presence of the desired *env* gene and the absence of other changes. The *env* gene fragments were then subcloned into pLP-IRES2-EGFP (Clontech) using Cre-recombinase (Clontech) in accordance with the manufacturer's instructions. 293T cells were cotransfected with pRSV-Rev (0.5 μg) and pLP-IRES2-EGFP-MOKW (9.5 μg) using the Effectene transfection reagent. After 36 h, the cells were harvested, incubated with each anti-HIV-1 MAb in combination with biotin-conjugated anti-human IgG and peridinin chlorophyll protein-conjugated streptavidin (BD Pharmingen), gated for the green fluorescent protein (GFP)-positive area, and analyzed using a FACSCalibur flow cytometry system.

MAb-gp120 binding assay. Culture supernatants containing the pseudotyped viruses were treated with 1% nonionic Nonidet P-40 to provide a source of gp120. Binding assays for MAbs to gp120 were then performed essentially as described elsewhere (41, 59). Briefly, gp120 proteins from transfected culture supernatants, diluted in Tris-buffered saline containing 10% FCS and 1% Nonidet P-40, were captured onto solid phase via their carboxyl termini using sheep polyclonal antibody D7324 (Aalto Bioreagents, Dublin, Ireland). MAb was added in PBS containing 10% FCS and 0.1% nonionic detergent Tween 20, and bound MAb was detected with alkaline phosphatase-conjugated goat anti-human IgG (Sigma) followed by the addition of phosphatase substrate (Sigma). A_{405} measurements were taken using a microplate reader.

Construction of chimeric NL4-3/MOKW *env* proviruses. Chimeric proviruses were constructed from the pNL4-3 proviral plasmid (AIDS Research and Reference Reagent Program, National Institute of Allergy and Infectious Diseases) by overlapping PCR as previously described, with minor modifications (31). Briefly, the gp160 coding sequences were amplified from the cloning vectors using the primers EnvFv (5′-AGCAGAAGACAGTGGCAATGAGAGCGAAG-3′) and EnvR (5′-TTTTGACCACTTGCCACCCATCTTATAGC-3′). A portion of the NL4-3 provirus from nucleotides 5284 to 6232 was amplified with primers NL(5284)F (5′-GGTCAGGGAGTCTCCATAGAATGGAGG-3′) and NL(6232)Rv (5′-CTTCGCTCTCATTGCCACTGTCTTCTGCT-3′). This fragment encompasses the unique EcoRI restriction site in pNL4-3. Another fragment from the NL4-3 provirus spanning nucleotides 8779 to 9045 was amplified using the primers NL(8779)F (5′-GCTATAAGATGGGTGGCAAGTGGTCAAAA-3′) and NL(9045)R (5′-GATCTACAGCTGCCTTGTAAGTCATTGGTC-3′). This fragment includes the unique XhoI restriction site in pNL4-3. Overlapping PCR was used to join the gp160 coding sequence from the desired clone to the fragment encompassing bases 8779 to 9045 that had been amplified from pNL4-3. The resulting fragment was then similarly joined to the amplified fragment encompassing bases 5284 to 6232 from pNL4-3. The product was digested with EcoRI and XhoI and subcloned into the corresponding site in pBluescript SK(+) (Stratagene) for sequencing and subsequent manipulation. The EcoRI-XhoI fragment for each *env* gene was then subcloned back into pNL4-3. The results were proviral plasmids that differed from each other only in the *env* gene. The resulting plasmids were designated pNL-MOKW-RDL and pNL-MOKW-KNL.

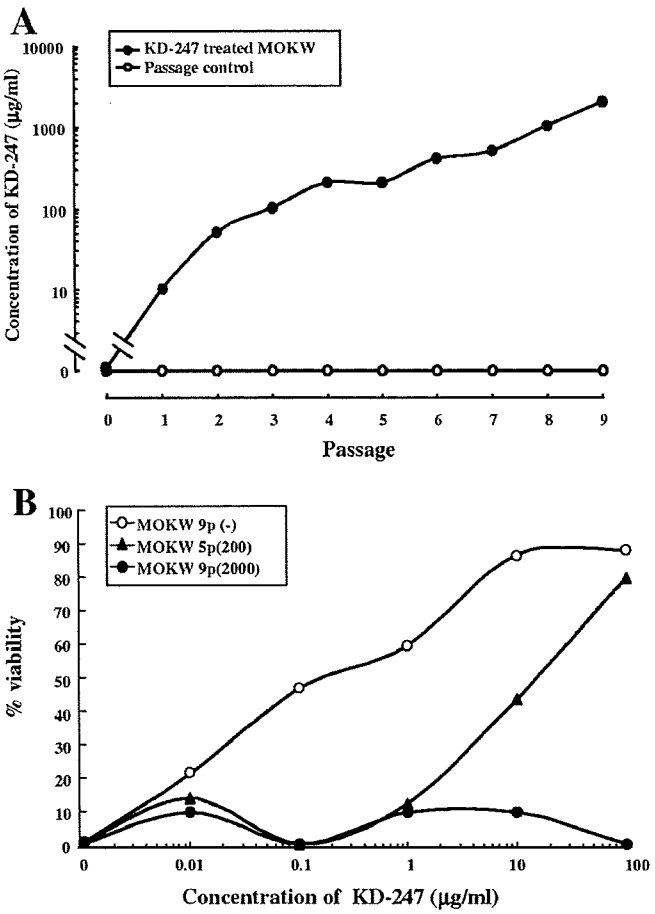

FIG. 1. Selection of neutralization-resistant virus variants against KD-247. (A) The selection was carried out in PM1/CCR5 cells, as described in Materials and Methods. (B) Sensitivity of MOKW5p(200) and MOKW9p(2000) virus to KD-247 as determined by MTT assay. PM1/CCR5 cells (2×10^3) were exposed to 100 $TCID_{50}$ of MOKW9p(−), MOKW5p(200), or MOKW9p(2000) virus and were cultured in the presence of various concentrations of KD-247. The IC_{50} values were determined by MTT assay on day 7 of culture. The assay was conducted in duplicate. The values shown are representative of three separate experiments.

Virus preparation and viral replication assay in PM1/CCR5 cells. Three micrograms of pNL-MOKW-RDL or pNL-MOKW-KNL was transfected into 293T cells using the Effectene transfection reagent. At 24 h after transfection, the virus-containing supernatants were harvested, filtered through a 0.2-μm-pore-size filter, and frozen in aliquots at −150°C. Viral yields were quantified by a RETROtek HIV-1 p24 antigen enzyme-linked immunosorbent assay (ELISA) kit (ZeptoMetrix). PM1/CCR5 cells (1×10^4) were exposed to NL4-3/MOKW *env* chimeric viruses corresponding to 10 ng of p24 and then preincubated for 4 h at 37°C. After incubation, cells were pelleted down and resuspended in RPMI 1640 medium supplemented with 10% FCS. Viral replication was monitored by measuring p24 kinetics in duplicate.

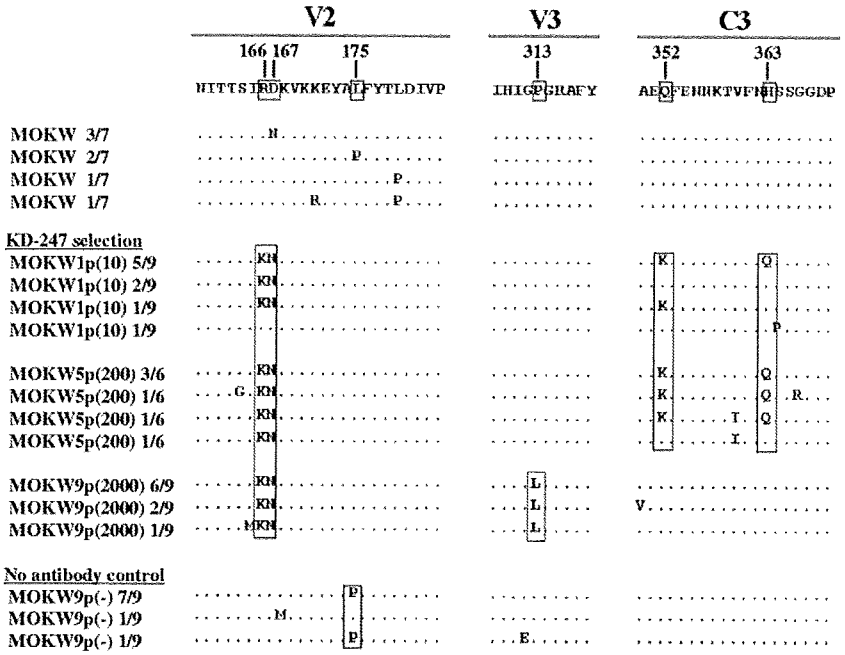

FIG. 2. Amino acid sequences of gp120 from the supernatants of MOKW-infected PM1/CCR5 cells passaged in the presence or absence of KD-247. Viral RNA from the cell culture supernatants at several concentrations of KD-247 was reverse transcribed. After the obtained cDNAs were subjected to PCR amplification and cloning, the *env* regions in the viruses passaged in the presence or absence of KD-247 were sequenced. The V2, V3, and C3 regions are indicated. The top amino acid sequence represents one of the major sequences from supernatants of MOKW-infected PBMCs. The locations and numbers of specific amino acids, based on the HXB2 sequence, are shown above the consensus line. The number of clones with the listed sequence among the total number of clones tested is given after each designation. For each set of clones, the deduced amino acid sequence of the gp120 was aligned by the single amino acid code. Dots denote sequence identity.

Nucleotide sequence accession numbers. Nucleotide sequences have been deposited in the DNA Data Bank of Japan under accession numbers AB262847 to AB262951 (passaged samples) and AB262952 to AB262961 (*env* expression vectors).

RESULTS

Anti-HIV-1 activity of KD-247 for the primary R5 isolate, MOKW virus. KD-247 recognized an epitope that contains the IGPGR sequence located at the tip of V3 and neutralized primary HIV-1 in clade B with matching sequence motifs (11). To study how bulked primary R5 virus can escape from anti-V3 antibody, we selected a genetically heterogenous HIV-1 primary isolate, MOKW, rather than a molecular clone to allow escape mutants to be selected from a quasi-species pool as well as to be generated de novo. MOKW virus was isolated by standard PBMC culture from a drug-naïve Japanese patient infected with HIV-1 by heterosexual contact (36). The isolate was sensitive to neutralization by KD-247 with a 50% inhibitory concentration (IC_{50}) of 3.4 μg/ml, which is comparable to the IC_{50} values of the Ba-L, JR-FL, and 89.6 viruses (data not shown).

Selection of KD-247 escape mutants from MOKW virus. To select an HIV-1 variant that could escape neutralization by KD-247 in vitro, we exposed PM1/CCR5 cells to MOKW virus and serially passaged the virus in the presence of increasing concentrations of KD-247. PM1/CCR5 cells were highly sensitive to both X4 and R5 HIV infection and were accompanied by prominent syncytia (68). As a control, MOKW virus was passaged under the same conditions but without KD-247 to allow us to monitor spontaneous changes that occurred in the virus during prolonged PM1/CCR5 cell passaging. The selected virus was initially propagated in the presence of 10 μg/ml KD-247, and during the course of the selection procedure, the MAb concentration was increased to 2,000 μg/ml (Fig. 1A). After five rounds of passaging, a viral variant, designated MOKW5p(200), arose that replicated in the presence of 200 μg of KD-247 per ml. Moreover, after nine rounds of passaging, a viral variant, designated MOKW9p(2000), arose that infected PM1/CCR5 cells efficiently in the presence of 2,000 μg/ml KD-247 (Fig. 1A). We harvested each passaged virus and a passaged control virus, designated MOKW9p(−), and evaluated their sensitivity to KD-247 using the MTT assay (Fig. 1B). The IC_{50} values of KD-247 against the MOKW9p(−), MOKW5p(200), and MOKW9p(2000) viruses were 0.15 μg/ml, 16 μg/ml, and >100 μg/ml, respectively, indicating that MOKW virus had acquired a resistance phenotype against KD-247 during the in vitro selection.

Sequences of the envelope region of the KD-247 escape mutants. To determine the genetic basis underlying the resistance of the variant MOKW strains, the *env* gene was amplified and sequenced. The C1 to C4 regions of the envelope were sequenced after cloning the PCR product for each region using cDNAs synthesized from viral RNAs obtained from the supernatants of infected cells, as previously described (67). A total of six to nine clones for each sample from PCR products from the passaged viruses were isolated and sequenced.

Before selection by KD-247 was begun, the V2 regions of MOKW *env* had variable amino acid sequences (Fig. 2). In

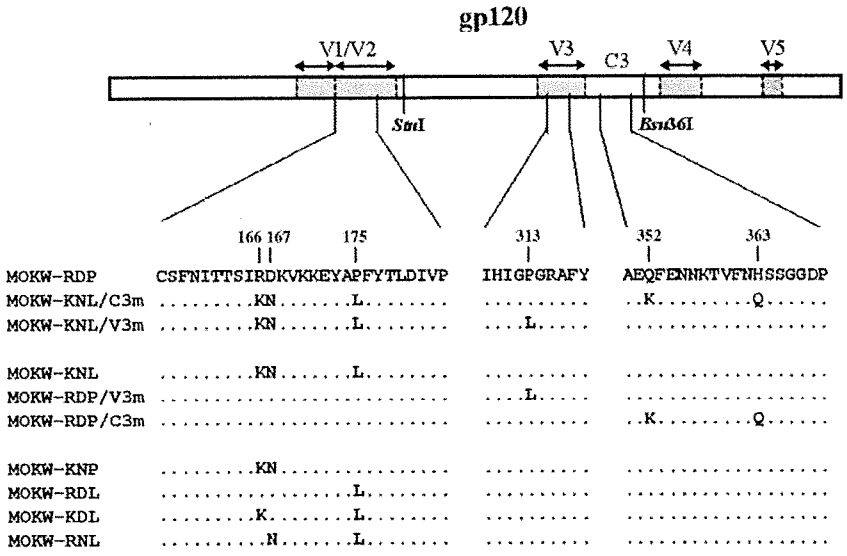

FIG. 3. Schematic representation of recombinant MOKW *env* genes used for analysis of the genetic basis for resistance to KD-247. MOKW-RDP, MOKW-KNL/C3m, and MOKW-KNL/V3m *env* genes were amplified from passaged MOKW virus-infected PM1/CCR5 cells in the absence or presence of KD-247. MOKW-KNL, MOKW-RDP/V3m, and MOKW-RDP/C3m *env* genes were constructed by replacing each region of MOKW-RDP with the corresponding MOKW-KNL/C3m or MOKW-KNL/V3m sequence. MOKW-KNP, MOKW-RDL, MOKW-KDL, and MOKW-RNL viruses were constructed by site-directed mutagenesis. Construction of the clones and mutagenesis procedures are described in Materials and Methods. The locations and numbers of specific amino acids, based on the HXB2 sequence, are shown above the MOKW-RDP sequence.

the first passage, two amino acid mutations in the V2 region and two amino acid mutations in the C3 region (five of nine clones) appeared, and after the fifth passage, the ratios of V2 and C3 mutated variants had further increased (seven of eight clones). However, after the ninth passage, the C3 mutations had completely disappeared, and a Pro-to-Leu substitution (P313L) in the V3 tip emerged in addition to the mutations in the V2 region (Fig. 2). The appearance of escape mutants with a V3 tip mutation was anticipated, because prior studies on the profile of KD-247 binding to peptides suggested that amino acid substitution at the V3 tip abrogates MAb binding (11). Some changes in the envelope sequence in other regions, including C1, V1, C2, V4, and C4, of the escape mutant were found even at early time points in the presence of the selective pressure. It is possible that these mutations also confer resistance to KD-247 but lead to viruses with decreased fitness, and thus they did not expand in the subsequent passage (Fig. 2 and data not shown). The virus passaged in PM1/CCR5 cells without KD-247 did not show the P313L substitution at passage 9 (zero of nine clones) (Fig. 2). However, accumulation of a mutation of leucine to proline at position 175 (L175P) in the V2 region was observed in the culture without KD-247. This mutation was not found in any passaged variants with KD-247.

Neutralization sensitivities of mutated MOKW pseudoviruses. To determine which substitutions were responsible for KD-247 resistance, we constructed luciferase-reporter viruses which were pseudotyped with the representative envelopes of MOKW5p(200), MOKW9p(2000), and passaged viruses without KD-247 [MOKW9p(−)], and were designated MOKW-KNL/C3m, MOKW-KNL/V3m, and MOKW-RDP virus, respectively (Fig. 3). Chimeric envelopes were constructed by replacing the mutated-region (V2, V3, or C3) with a corresponding MOKW-RDP virus (designated MOKW-KNL, MOKW-RDP/V3m, and MOKW-RDP/C3m, respectively), and then sensitivity was compared with that of the passaged virus without KD-247. As shown in Fig. 4, the V3-tip-mutated pseudoviruses, MOKW-KNL/V3m and MOKW-RDP/V3m, were completely resistant to KD-247 (>25,000-fold), whereas V2-mutated viruses, MOKW-KNL/C3m and MOKW-KNL, were only partially resistant (125-fold and 500-fold, respectively) (Fig. 4 and Table 1). The involvement in neutralization resistance of mutation in the V1/V2 region has been reported by number of researchers (12, 49, 50, 54). Our results show that the MOKW variants that had V2 mutations and a resistance phenotype against KD-247 were selected under pressure from relatively low concentrations of KD-247 (10 to 200 μg/ml) and that evolution of fully resistant variants with a mutation in the V3 tip was observed under pressure from high concentrations of the antibody.

We then determined whether the KD-247 escape variants remained sensitive to other neutralizing antibodies (447-52D and 17b), rsCD4, anti-CCR5 antibody (2D7), anti-CD4 antibody (RPA-T4), and the small-molecule CCR5 inhibitor (TAK-779) (Fig. 4 and Table 1). The KD-247 escape variants with the P313L mutation, MOKW-KNL/V3m and MOKW-RDP/V3m, were also resistant to another anti-V3 MAb, 447-52D, and V2-mutated viruses without V3 mutation, MOKW-KNL/C3m and MOKW-KNL, were partially resistant (the same as for KD-247). In contrast, the V2-mutated viruses (MOKW-KNL/C3m, MOKW-KNL/V3m, and MOKW-KNL) showed resistance to rsCD4 and 17b (a MAb to the CD4-induced epitope; CD4i) compared with the pseudoviruses without V2 mutations, i.e., MOKW-RDP, MOKW-RDP/C3m, and MOKW-RDP/V3m. Moreover, the pseudoviruses with V3 tip mutations, MOKW-KNL/V3m and MOKW-RDP/V3m, be-

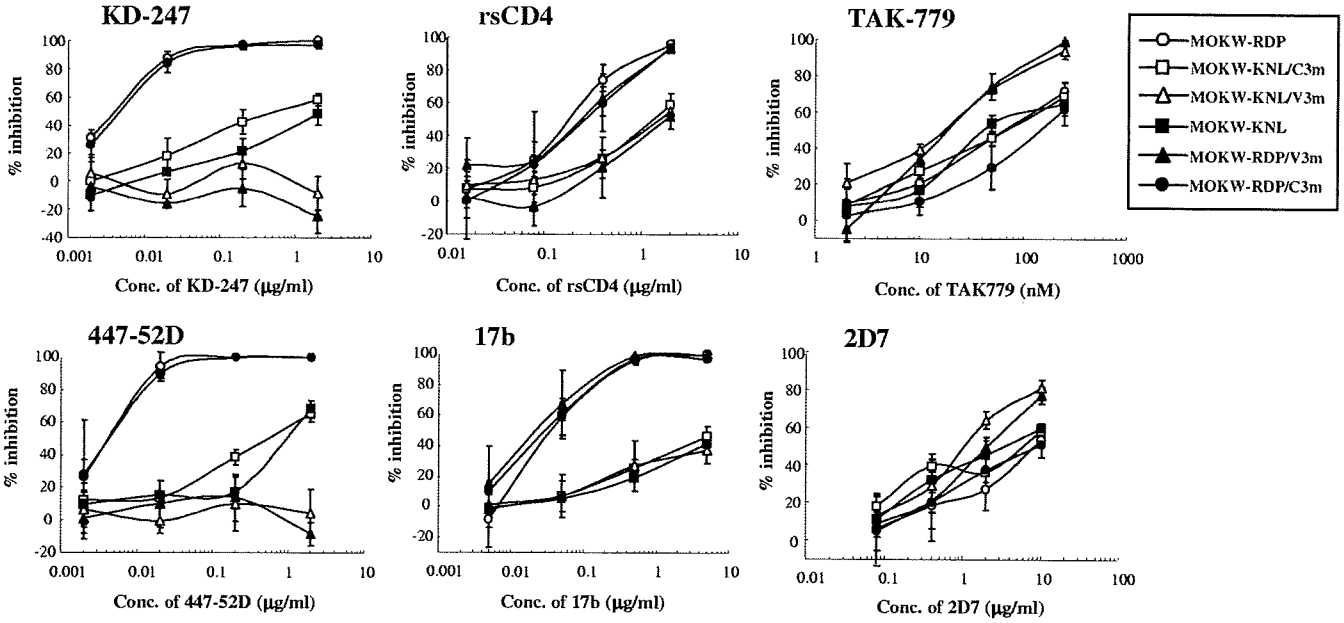

FIG. 4. Neutralization sensitivities of pseudoviruses with *env* genes from passaged MOKW viruses to MAbs, rsCD4, and CCR5 inhibitors. Pseudoviruses with the envelope sequences listed on the figure were prepared as described in Materials and Methods. KD-247, 447-52D, rsCD4, and 17b were preincubated with 100 $TCID_{50}$ of each MOKW pseudotype virus for 15 min, followed by the addition of the mixtures to the target cells (GHOST-hi5). The target cells were treated with TAK-779 and 2D7 for 15 min, followed by inoculation of the pseudotype clones. The inhibitory effects were determined by measuring the luciferase activities on day 2 of culture. Conc, concentration.

came significantly more sensitive to TAK-779 and 2D7 compared with pseudoviruses without the P313L mutation (Fig. 4 and Table 1). No significant differences with respect to sensitivity to RPA-T4 were observed between any pseudoviruses (Table 1). These data indicate that V3 tip and V2 mutations confer neutralization resistance against anti-V3 antibodies and that these mutations affect viral sensitivity to neutralizing antibodies recognizing different epitopes and anti-CCR5 antibody/agents.

Binding affinity of neutralizing antibodies to MOKW Env proteins on the cell surface. To elucidate the mechanism by which escape virus variants with V3 tip and V2 mutations become less sensitive to neutralizing antibodies, MOKW Env-expressing 293T cells were established by transfection with each Env expression plasmid and then stained with the MAbs. Binding of KD-247, 447-52D, and 17b to the surface-expressed Env proteins was assayed using fluorescence-activated cell sorter (FACS) analysis. As shown in Fig. 5A, the mean fluorescence intensities (MFIs) of KD-247 binding to the Env proteins without either V2 or V3 mutations (the MOKW-RDP and MOKW-RDP/C3m cells) were 30.13 and 29.20, respectively. However, the corresponding values for the V3-tip-mutated Env-expressing cells (MOKW-KNL/V3m and MOKW-RDP/V3m) were almost the same as negative controls (6.90 and 6.66, respectively). The MFI of the V2-mutated Env-expressing cells (MOKW-KNL/C3m and MOKW-KNL) indicated a lower binding affinity (17.89 and 19.18, respectively) than for Env proteins without V2 and V3 mutations. The binding pattern of 447-52D to these Env-expressing cells was similar to that of KD-247 (Fig. 5B). However, reduction in the binding of 17b was observed for strains with V2-mutated Env proteins (MOKW-KNL/C3m, MOKW-KNL/V3m, and

TABLE 1. Anti-HIV-1 activities of various MAbs and inhibitors toward MOKW pseudoviruses

Class	Compound	IC_{50} (μg/ml) of the indicated virus (relative IC_{50})[a]					
		MOKW-RDP	MOKW-KNL/C3m	MOKW-KNL/V3m	MOKW-RDP/C3m	MOKW-KNL	MOKW-RDP/V3m
V3 MAbs	KD-247	0.004 (1)	0.5 (125)	>100 (>25,000)	0.005 (1.3)	2 (500)	>100 (>25,000)
	447-52D	0.004 (1)	0.5 (125)	>2 (>500)	0.004 (1)	0.8 (200)	>2 (>500)
CD4-induced MAb	17b	0.035 (1)	>5 (>143)	>5 (>143)	0.03 (0.86)	>5 (>143)	0.02 (0.57)
CD4	rsCD4	0.18 (1)	1.3 (7.22)	1.5 (8.33)	0.24 (1.33)	1.8 (10)	0.24 (1.33)
CCR5 MAb	2D7	8 (1)	6.8 (0.85)	1 (0.13)	8 (1)	3.2 (0.4)	2 (0.25)
CCR5 inhibitor	TAK-779	63 (1)	63 (1)	18 (0.29)	140 (2.22)	65 (1)	18 (0.29)
CD4 MAb	RPA-T4	0.4 (1)	0.26 (0.65)	0.22 (0.55)	0.5 (1.25)	0.22 (0.55)	0.44 (1.1)

[a] GHOST-hi5 cells were exposed to 100 $TCID_{50}$ of each MOKW pseudovirus and then cultured in the presence of various concentrations of MAb or inhibitors. The IC_{50} values were determined using the luciferase reporter assay on day 2 of culture. All assays were conducted in triplicate. The value in parentheses is the ratio of the IC_{50} of the compound to the IC_{50} of the MOKW-RDP virus. Values for the compound TAK-779 are nanomolar concentrations. Data shown are representative of two or three separate experiments.

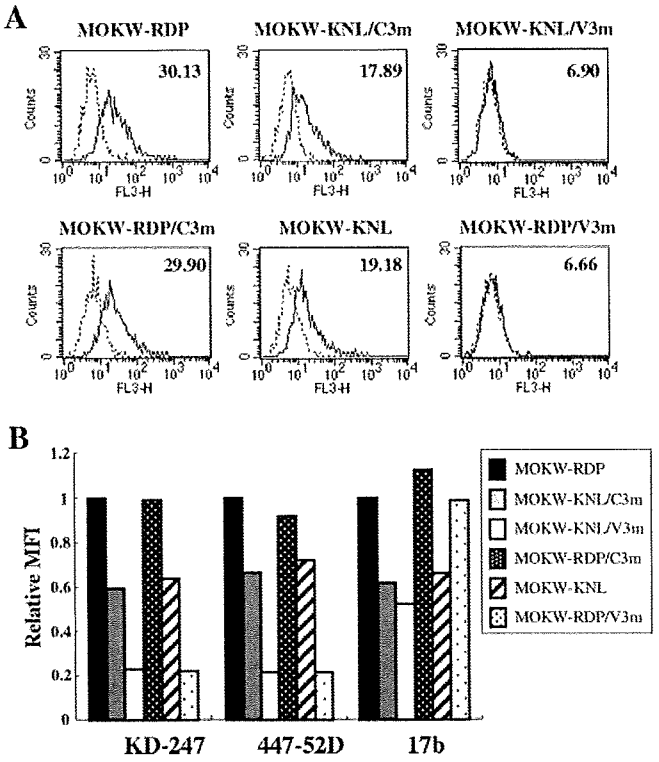

FIG. 5. Comparison of antibody binding to cell surface-expressed MOKW Env proteins. (A) 293T cells transfected with MOKW Env expression vectors were harvested at 24 h posttransfection and stained with KD-247. Flow cytometry data for binding of the KD-247 (black lines) to cell surface MOKW Env proteins are shown among GFP-gated 293T cells along with the control antibody (normal human IgG; dotted lines). The number at the top right of each graph is the MFI. (B) Each bar indicates the relative binding of KD-247, 447-52D, and 17b to MOKW Env-expressing cell surfaces. Data were normalized to each antibody's MFI for MOKW-RDP virus. FL3-H, relative fluorescence.

MOKW-KNL), whereas no difference in 17b binding was noted for the V3-mutants without V2 mutations (Fig. 5B). These findings are consistent with the results of a single-round neutralization assay (Fig. 4). Taken together, these data suggest that the mutations in V2 have a significant influence on access by antibodies to V3 as well as to the CD4i epitope. This is because access by antibodies to the epitopes of the functional envelope is related to neutralization sensitivity or resistance.

Identification of the V2 region site responsible for the neutralization resistance phenotype by site-directed mutagenesis of specific residues. Because KD-247 recognizes an epitope containing the IGPGR amino acid sequence in the V3 tip, the MAb could not bind the V3 tip of mutated Env proteins. Consequently, KD-247 does not neutralize V3-tip-mutated virus strains (67). However, the mechanism of neutralization resistance associated with V2 mutations is not known. To clarify the responsible mutation in the V2 region that confers the escape phenotype with respect to KD-247, we introduced V2 amino acid changes individually and in combination into the MOKW-RDP Env expression vector (Fig. 3) and measured the sensitivities of pseudoviruses with these envelopes to KD-247. As shown in Fig. 6, the R166K/D167N double mutant, MOKW-KNP virus, showed almost the same neutralization sensitivity as MOKW-RDP virus against KD-247. Surprisingly, a single amino acid change (P175L in MOKW-RDL) was sufficient to confer >10,000-fold resistance upon MOKW-RDP virus, with an IC_{50} of >100 μg/ml. R166K/P175L (MOKW-KDL) mutations also conferred resistance. Both the MOKW-RDL and MOKW-KDL viruses were much more resistant than the fully V2-mutated virus, MOKW-KNL (>100-fold and >10-fold resistance, respectively) (Fig. 6). The D167N/P175L (MOKW-RNL) mutant was more resistant than MOKW-KNL virus (10-fold) but less resistant than the MOKW-RDL and MOKW-KDL viruses. We also constructed a V2 mutant of JR-FL and confirmed that JR-FL with an amino acid substitution of Leu to Pro at position 175 became highly sensitive to KD-247 compared with JR-FL with Leu at position 175 in Env (data not shown). These results suggest that residue 175 (Pro or Leu) is the crucial amino acid for determining neutralization sensitivity against KD-247 and that the phenotypic influence of the R166K and D167N changes is strictly context dependent, requiring the presence of Leu at residue 175.

We then determined whether these pseudoviruses with various V2 mutations remained sensitive to other neutralizing antibodies (447-52D and IgGb12), rsCD4, 2D7, RPA-T4, and TAK-779 (Fig. 6). MOKW-RDL and MOKW-KDL viruses were also resistant to another anti-V3 MAb, 447-52D, CD4 binding site MAb, IgGb12, and rsCD4. MOKW-RNL was partially resistant compared with MOKW-KNL but less resistant than MOKW-RDL and MOKW-KDL against 447-52D, IgGb12, and rsCD4. These results were similar to those for KD-247. All V2-mutated clones were sensitive to TAK-779 and 2D7, as was MOKW-RDP virus (Fig. 6 and data not shown). However, the anti-CD4 MAb RPA-T4 neutralized both the MOKW-RDL and MOKW-KDL viruses at an approximately threefold lower concentration than other viruses (Fig. 6). These results suggest that the amino acids at positions 166 and 167 (with RD and KN sequences) may help compensate for any reduced fitness of viruses with Leu at residue 175. On the other hand, Pro at position 175 in MOKW-RDP virus might be accumulated because it confers better fitness to replicate on PM1/CCR5 cells in the absence of KD-247 pressure.

Binding affinity of MAbs against monomeric or cell surface-expressed gp120 with mutations in V2. To determine the difference in binding of MAbs to monomeric gp120 of MOKW Env with V2 mutations relative to that of MOKW-RDP virus, we performed MAb binding assays. Monomeric gp120 was prepared from pseudoviruses that had a series of V2 mutations and was captured on an ELISA plate, followed by detection by MAbs. No difference was noted in the binding activity of KD-247 or 447-52D to monomeric gp120 from V2-mutated and MOKW-RDP envelopes (Fig. 7). These results suggest that V2-mutated Env proteins retain the neutralizing epitope at least in monomeric gp120.

In contrast to the monomeric form, gp120 expressed on the cell surface contained, to a certain degree, functional envelope oligomers that were directly related to the infectivity and neutralization sensitivity of the virus. To compare the binding activity of MAbs for the surface-expressed Env with the results obtained for monomeric gp120, 293T cells transfected with MOKW-RDP and MOKW-KNP viruses, a V2 mutant strain, were subjected to FACS analysis. As shown in Fig. 8A and B,

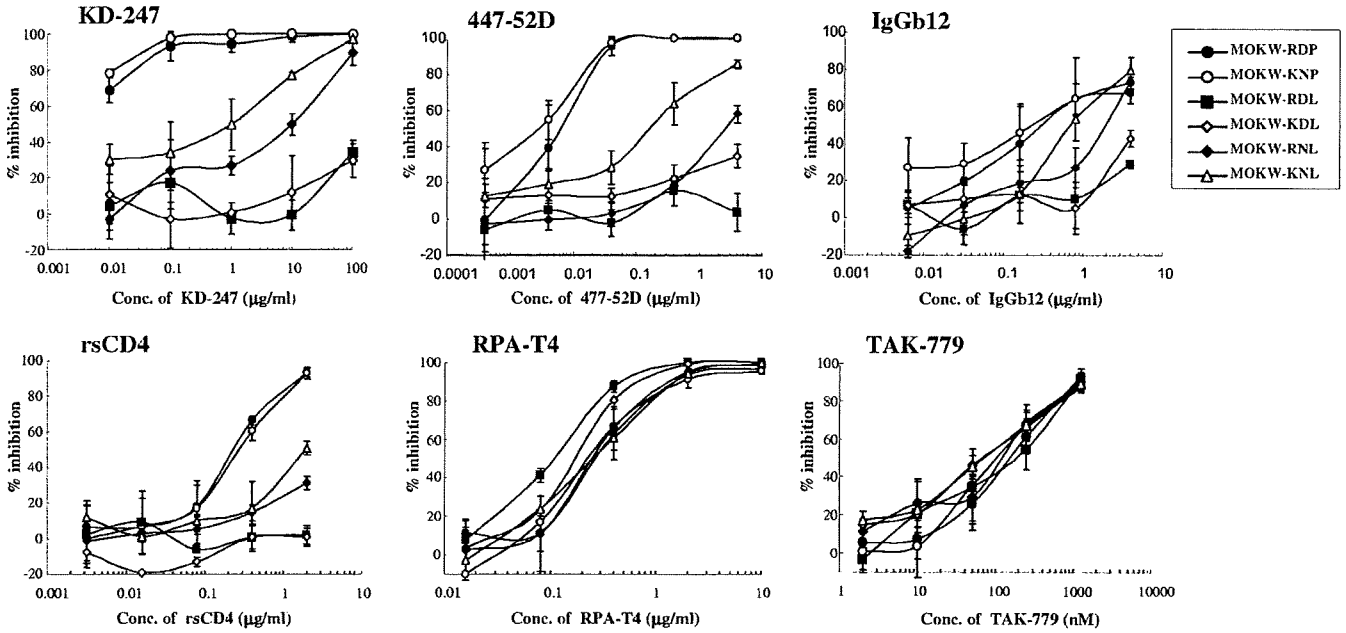

FIG. 6. Neutralization sensitivities of pseudoviruses with *env* genes from MOKW9C(−) virus with selected V2 mutations to MAbs, rsCD4, and CCR5 inhibitors. Pseudoviruses that have envelope sequences with the selected V2 mutations listed on Fig. 4 were prepared as described in Materials and Methods. KD-247, 447-52D, rsCD4, and IgGb12 were preincubated with 100 $TCID_{50}$ of each MOKW pseudotype virus for 15 min, followed by addition of the mixtures to the target cells (GHOST-hi5). Target cells were treated with TAK-779 and RPA-T4 for 15 min, followed by inoculation of the pseudotype clones. Inhibitory effects were determined by measuring the luciferase activities on day 2 of culture. Conc, concentration.

the relative binding of KD-247, 447-52D, and IgGb12 to Env expressed on the cell surface was no different than for MOKW-RDP and MOKW-KNP.

Consistent with the results of the single-round neutralization assay shown in Fig. 6, MOKW-RDL virus had the lowest binding affinity for all tested MAbs. To determine which mutations (166K or 167N) further influence binding affinity, in addition to the MOKW-RDL background, we constructed MOKW-KDL and MOKW-RNL Env proteins and measured the binding affinity by FACS. The MOKW-KDL Env was found to have a slightly greater binding affinity for KD-247, 447-52D, and IgGb12 than MOKW-RDL Env. But cell surface binding of all tested MAbs to MOKW-RNL was better than for MOKW-KDL. The strain with a fully V2-mutated Env, MOKW-KNL, had a binding profile that was intermediate between single- or double-mutated Env proteins and nonmutated Env, but in the case of IgGb12, the binding affinity of MAbs for MOKW-KNL was comparable to that for MOKW-RDP. These data were consistent with the results obtained from the neutralizing assay using a high concentration of each MAb (Fig. 6).

Comparison of replication kinetics between the NL-MOKW-RDL and NL-MOKW-KNL viruses. Although the MOKW-RDL variant was much more resistant against KD-247 than the MOKW-KNL variant (Fig. 6) and the RD sequence was

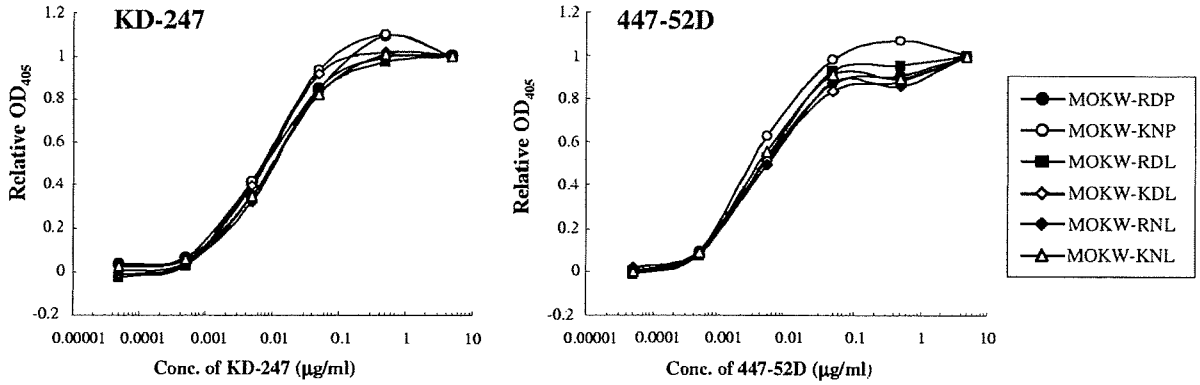

FIG. 7. Binding affinity of anti-V3 MAbs to monomeric gp120. Viral lysates for each MOKW pseudovirus were used. gp120 was captured onto microtiter wells using a sheep polyclonal antibody specific for the C terminus of gp120. Serial dilutions of KD-247 or 447-52D were tested for binding by ELISA. Because of differences in the amount of bound gp120, optical density at 405 nm (OD_{405}) values were normalized to saturating levels of antibody (5 μg/ml) for comparison. Conc, concentration.

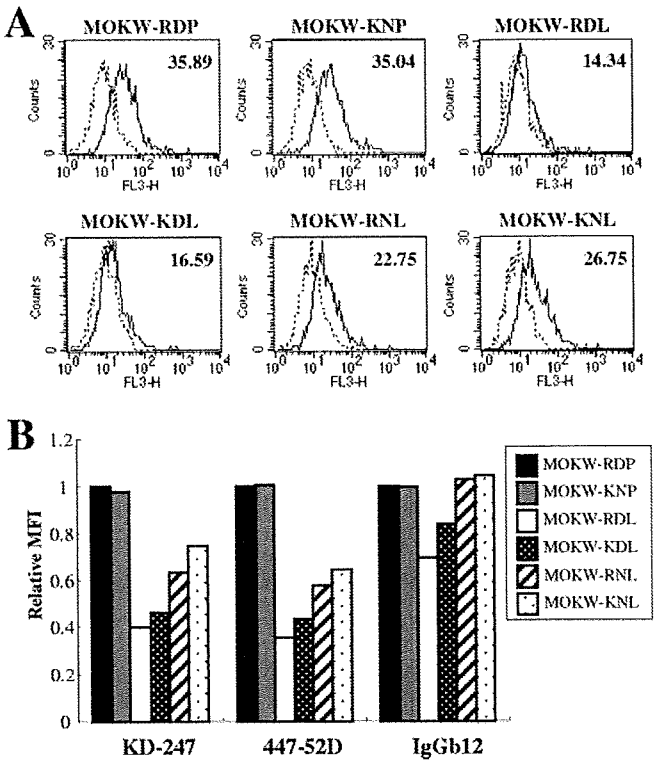

FIG. 8. Comparison of antibody binding to cell surface-expressed MOKW Env proteins with V2 mutations. (A) 293T cells transfected with MOKW Env-expression vectors were harvested at 24 h posttransfection and stained with KD-247. Flow cytometry data for binding of the KD-247 (black lines) to cell surface MOKW Env proteins are shown for GFP-gated 293T cells along with data for the control antibody (normal human IgG; dotted lines). The number at the top right of each graph is the MFI. (B) Each bar indicates relative binding of KD-247, 447-52D, and IgGb12 to MOKW Env-expressing cell surfaces. Data were normalized to each antibody's MFI for MOKW-RDP virus. FL3-H, relative fluorescence.

more prevalent than KN at positions 166 and 167 in the V2 region before selection (Fig. 2), the MOKW variants with 166K/167N/175L were selected and outgrown under KD-247 pressure (Fig. 2). It was possible that the KN sequences at positions 166 and 167 are necessary to compensate for the fitness of the variants with 175L in PM1/CCR5 cells, as shown in Fig. 6. To clarify the role of KN at positions 166 and 167 in replication, we constructed replication-competent viruses with a MOKW Env with RD or KN in addition to 175L (NL-MOKW-RDL and NL-MOKW-KNL) and compared their replication kinetics. As shown in Fig. 9, NL-MOKW-KNL virus replicated faster than NL-MOKW-RDL virus in PM1/CCR5 cells. These data suggested that KN sequences at positions 166 and 167 with the 175L variant confer a replication advantage in PM1/CCR5 cells. Therefore, the intermediate-resistant variant MOKW virus with the KNL sequence in the V2 region might replicate more rapidly than the highly resistant variant MOKW virus with RDL against KD-247 in the course of selection.

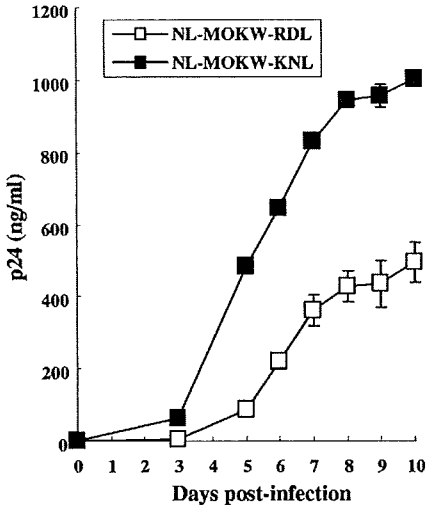

FIG. 9. Replication kinetics of infectious molecular clones NL-MOKW-RDL and NL-MOKW-KNL. PM1/CCR5 cells were exposed to NL-MOKW-RDL (open square) or NL-MOKW-KNL (filled square) and cultured for 10 days. Virus replication was monitored by measuring the amounts of p24 Gag protein produced in the culture supernatants. The data are representative of the results from two independent experiments.

DISCUSSION

Although an attack from the humoral immune response, especially anti-V3 NAb, is lasting against HIV-1 in vivo, it is not clear why the V3 tip sequence is conserved in the course of the infection. In the present study, by using a genetically heterogeneous HIV-1 primary R5 isolate, MOKW virus, we found that V2- and C3-mutated viruses expanded under conditions with a relatively low concentration of KD-247. Further, we found that the V3-tip-mutated virus was induced only under conditions with a high concentration of MAb (more than 500 μg/ml). Using region-swapping analysis, it was found that both V2 and V3 tip mutations can cause an escape phenotype against anti-V3 antibody. Neutralization escape variants with V2 mutations could be selected from quasi-species existing in the primary isolate at relatively low antibody pressures. On the other hand, highly resistant variants with amino acid substitutions in the V3 epitope emerged via evolution of the virus in the presence of a high concentration of the MAb.

The V1/V2 region of gp120 is highly diverse, not only in respect to virus subtypes but also in respect to intraspecies diversity in the same patient (16, 61, 66). The primary isolate, MOKW, also displayed diversity in the V2 region (Fig. 2), and the first-passaged virus already harbored mutations in the V2 region. Many researchers have reported that the V1/V2 domain strongly influences neutralization of the anti-V3 MAbs, MAbs to the other epitopes, and rsCD4 (12, 13, 25, 27, 30, 44, 49, 50). Moreover, structural models of the Env trimer have been proposed that place the base of the V1/V2 loop of one subunit in proximity to the V3 loop of a neighboring subunit (32, 34). In the present study we observed a reduction in the binding of anti-V3 MAbs to V2-mutated Env expressed on the cell surface, whereas mutations in V2 did not have an effect on the binding of the MAbs to monomeric gp120. These results suggest the association of V2 mutations with anti-V3 antibody

accessibility in the context of the oligomeric conformation of the functional envelope. It has been proposed that the gp120 of T-cell-line-adapted strains forms a relatively open conformation and that the primary isolate trimeric complex has a more closed conformation (2, 51). These findings suggest that antibody-induced V2 mutations may affect envelope oligomers on the viral surface so that they form a more closed conformation; thus, neutralization epitopes become less accessible to antibodies. The essential amino acid residues responsible for neutralization resistance located at the center of the V2 region may have a role in the interaction with the V3 loop of neighboring gp120 molecules.

We previously described the in vitro selection and characterization of a KD-247-escape mutant of JR-FL (67). The amino acid substitution that was critical for the resistance phenotype was Gly to Glu at residue 314 (G314E) in the V3 tip region. The genetically engineered mutant was completely resistant to neutralization by KD-247. Other researchers have also reported the induction of V3-mutated viruses by strain-specific anti-V3 MAb in in vitro culture systems (8, 37, 65). In earlier studies, combinations of genetically cloned viruses and highly potent NAbs were used for in vitro selection (8, 37, 65). The escape mutants were induced in the presence of high concentrations of MAbs to acquire V3 tip mutation(s). In contrast to these observations in vitro, the Gly-Pro-Gly amino acid sequence in the V3 tip varies to a negligible extent in clinical isolates from HIV-1-infected patients (35). The important role of the V3 tip in forming the β-turn of the V3 loop and in interacting with chemokine receptors may partly explain the discrepancy between in vivo and in vitro studies (19). In addition to the V3 loop, variation in or near the V1/V2 region is known to contribute to coreceptor usage of HIV-1 (17, 21, 27, 28, 47, 56, 64, 66). However, it is possible that HIV-1 suffers critical damage with respect to replication and infectivity through mutation in the V3 region, especially in the tip region, because the V3 loop plays a major role in the interaction of gp120 with coreceptors. Thus, mutations in the V2 region may be important not only to avoid anti-V3 pressure but also to maintain replication efficiency at a suitable level.

In the present study, which used a MOKW primary virus for selection, the virus underwent acquisition of resistance via V2 mutations and then V2 plus V3 mutations in response to increases in the concentration of MAb. By contrast, no V2 mutations were selected in JR-FL by KD-247 pressure in our previous study (67). Because MOKW was a primary isolate, the viruses contained quasi-species of related but distinct viruses, and relatively resistant variants with mutations in V2 were easily selected for replication. Pinter et al. found that inherent neutralization resistance in JR-FL is mediated by the V1/V2 domain (50). It is therefore possible that the V1/V2 sequence (or the conformation of this sequence) in JR-FL already had a resistance phenotype against anti-V3 antibodies because the escape variant underwent mutation directly in the V3 tip of the KD-247-reacting epitope (67).

In the in vitro selection process, amino acid residue 175 (Pro or Leu) in the V2 region of MOKW virus played a crucial role in dramatically changing the oligomeric state of the envelopes. However, MOKW-RDP obtained by prolonged culture in vitro without KD-247 became neutralization sensitive compared with MOKW virus. Residue 175P was the amino acid responsible for the change to the neutralization-sensitive phenotype, whereas viruses with 175L became highly resistant to the MAbs and rsCD4. The same phenomenon was observed in the relatively resistant strain JR-FL. Residue 175L is highly conserved among HIV-1 strains and is located at the center of the V2 loop (35), and the V2 region also mediates gp41-independent intersubunit contact (5). It is therefore possible that the V2 region, including residue 175, by mediating changes in the conformation of the gp120 oligomer, contributes to resistance to neutralization by limiting the exposure of epitopes.

Although the MOKW-RDL virus had a highly resistant phenotype against KD-247, MOKW virus with R166K/D167N and P175L in the V2 region and with the C3 mutations, which were less neutralization resistant than MOKW-RDL virus, were expanded in in vitro selection. Substitutions at residues 165 to 167 during the adaptation of various HIV-1 strains to replication in vitro have been reported; the adaptation is associated with an increase of the positive charge of this amino acid motif (1, 13, 39, 52, 57, 63). In our present study, the amino acid change at 166/167 in the V2 region in passaged MOKW viruses with KD-247 was RD to KN, again increasing the positive charge. MOKW-RDL virus was partially sensitive to anti-CD4 MAb (RPA-T4) compared with MOKW viruses with 175P, MOKW-RDP, and other 166/167-mutated MOKW viruses. Pugach et al. also showed that charged amino acids at residues 165 to 167 with 175L in the V2 region emerged during in vitro replication and that these viruses also had their sensitivity to rsCD4 and resistance to the anti-CD4 antibody slightly changed by the charged amino acids at positions 165 to 167 (52). It is therefore possible that amino acid mutations at positions 166 and 167 are necessary to compensate variants with 175L for interactions with CD4 molecules on the target cell membrane. As shown in Fig. 9, KN sequences at positions 166 and 167 with the 175L variant confer replication advantage in PM1/CCR5 cells. Therefore, residues 166 and 167 may help compensate for the reduced fitness of the viruses with Leu at position 175 in PM1/CCR5 cells. C3 mutations may also be involved in a minor compensation effect in replication cycles under moderate selective pressure from KD-247 (45, 60).

The neutralization resistance of primary HIV-1 variants is considered instrumental for HIV-1 persistence in the presence of NAbs in vivo. Various immunological pressures always induce escape variants by eliciting appropriate mutation(s) (14, 60, 62). In the present study, we found that HIV-1 could escape from the broadly reactive anti-V3 MAb, KD-247, by stepwise mutation in the V2 and V3 regions. These observations strongly support the idea that the major problem facing the development of V3-based immunogens is not sequence variation within V3 but, rather, that access of most V3-directed antibodies to their epitopes in functional Env complexes is blocked, often by the V1/V2 domain (29, 50).

Our observations support the hypothesis that neutralization escape in a primary isolate is mainly mediated by amino acid substitutions in the V2 region in vivo, because only a moderate selective pressure by neutralizing antibodies against autologous viruses has been reported for infected individuals (9, 14, 26, 50, 62). The large sequence diversity observed for V2 in quasi-species existing in patients may represent the accumulation of escape mutants early in HIV-1 infection in response to NAb pressure. Our observations may also explain why the V3